

# Mechanisms in Molecular SIMS<sup>†</sup>

STEVEN J. PACHUTA and R. G. COOKS\*

Department of Chemistry, Purdue University, West Lafayette, Indiana 47907

Received December 18, 1986 (Revised Manuscript Received March 17, 1987)

## Contents

I. Introduction	647
II. Desorption Ionization Techniques	648
A. Secondary Ion Mass Spectrometry	648
1. Experimental Aspects	648
2. Spectral Characteristics of Molecular SIMS	648
B. Fast Atom Bombardment and Other Desorption Ionization Methods	649
III. Mechanistic Aspects of Atomic SIMS	650
A. Overview	650
B. Sputtering Models	651
C. Ionization	652
1. Qualitative Models	652
2. Semiquantitative Models	654
D. Additional Aspects of Atomic SIMS	655
IV. Mechanistic Aspects of Molecular SIMS	655
A. Overview	655
B. Collision Cascade Models	656
1. Classical Dynamics Model	656
2. Precursor Model	657
C. Thermal and Vibrational Models	658
V. Mechanistic Insights from Other Desorption Ionization Techniques	661
A. Mechanisms in FABMS and Liquid SIMS	661
B. Mechanisms in Other Desorption Ionization Techniques	662
C. Unified Description of Desorption Ionization	665

## I. Introduction

Secondary ion mass spectrometry (SIMS) and related desorption ionization (DI) techniques—fast atom bombardment mass spectrometry (FABMS), plasma desorption mass spectrometry (PDMS), and laser desorption mass spectrometry (LDMS)—are finding increasing use in molecular analyses of surfaces, including the characterization of large molecules prepared from condensed-phase samples. These methods have evolved over a relatively long period beginning with Grove's report in 1853 of cathode erosion by gaseous ions in a discharge source.<sup>1</sup> In 1910, Thomson investigated "the secondary Canalstrahlen produced when primary Canalstrahlen strike against a metal plate".<sup>2</sup> Over the next 50-odd years occasional papers on secondary atomic ion emission were published,<sup>3</sup> but it was not until the mid 1950s that sputtering progressed beyond the stage of being a curiosity and the seeds were sown for its use as an analytical technique.<sup>4,5</sup>

The physical basis for sputtering and ionization of solids by high-energy particles has intrigued researchers ever since Thomson's experiments. Knowledge of the



Steven J. Pachuta was born in 1959 in New Brunswick, NJ. He was raised on both coasts and in several places in between. In 1981 he received his B.S. in chemistry from the University of Georgia, and in 1986 he received his Ph.D. in analytical chemistry from Purdue University. His graduate research was conducted under the direction of Professor R. Graham Cooks in the areas of tandem mass spectrometry and secondary ion mass spectrometry. He is currently a Senior Chemist at 3M Co., St. Paul, MN, where he is involved with analytical chemistry of surfaces.



Graham Cooks is an analytical chemist who has spent his career in mass spectrometry. He introduced the method of tandem mass spectrometry (MS/MS) for analysis of mixtures. Current interests include polyatomic ion/surface collision phenomena and ion-trapping devices. He is chair of Purdue's Visual Arts Committee and a proponent of close academic/industrial research cooperation.

mechanisms of desorption ionization is important not only from a theoretical point of view but also from the perspective of increasing the analytical utility of the method. The DI mechanism suffers the stigma of being "not at all well understood".<sup>6</sup> For some years this type of statement has appeared in the literature. Progress has been made, however, and it will be helpful at the outset to touch upon current thinking in regard to the SIMS mechanism. In brief, no single mechanism tidily accommodates all the facts, but a qualitative description that is nonetheless useful has emerged. This paper attempts to bring together the extensive experimental data—often apparently contradictory—that provide insight into the molecular SIMS mechanism. It will be

<sup>†</sup>Dedicated to Rick Honig as he retires from a long career in SIMS.

seen that the mechanism is best described by processes involving conversion of the kinetic energy of the projectile through collision cascades<sup>7</sup> to a translationally and later a vibrationally excited interfacial region. The key to many observations are the *chemical* processes that occur in this region, a finding which was presaged by work on the mechanism of field desorption.<sup>8</sup>

The various desorption ionization techniques tend to produce very similar spectra. They give predominantly even-electron ions from large molecules, often with a limited degree of fragmentation. Similarities between the spectra obtained with incident beams of slow (keV) and fast (MeV) particles, and with photons, can be explained by a merging of mechanisms after the initial excitation process. It is reasonable to propose that a vibrationally excited, disturbed surface is the key feature. In the selvedge, as this region is sometimes known,<sup>9</sup> both ion/molecule and dissociation reactions can occur. In SIMS, there is little doubt that collision cascades are responsible for initial excitation of the system and that they lead directly to the emission of many of the ions and neutrals from certain systems—e.g., bulk metals and adsorbed gases on metals. Collision cascades probably establish the hot selvedge from which the emission of large molecules occurs by other mechanisms for organic samples. The fact that similar spectra are recorded in SIMS and in LD (where collision cascades can hardly be proposed) supports this.

The paper commences with descriptions of the major desorption ionization techniques. Since the types of ions generated by these techniques are very similar, information extracted from one technique can sometimes be used to elucidate aspects of another. An overview of atomic SIMS theory will be followed by a more detailed analysis of molecular SIMS, with emphasis on the experimental results and the different models that seek to accommodate them. The final section will attempt to clarify the important mechanistic features of various desorption ionization techniques.

## II. Desorption Ionization Techniques

### A. Secondary Ion Mass Spectrometry

#### 1. Experimental Aspects

Experimentally, SIMS is a simple technique. A primary ion beam, typically of keV energy, bombards a surface, and secondary ions sputtered from the surface are mass-analyzed. There exist a considerable number of variables in this method, however, including choice of primary ion, its kinetic energy and current density, the nature of the analyte, polarity of the secondary ions, collection and sputtering angles selected, type of analyzer, type of detector, and so on. Each of these factors can more or less significantly alter the mass spectrum. For example, the high primary ion currents encountered in atomic SIMS can cause gross chemical transformations in the sample. Hence, molecular SIMS is done by using low primary ion currents, or, alternatively, liquid, rather than solid, matrices. Most of the variables in the list above can also yield clues to the SIMS mechanism. Table I gives descriptions of many of these parameters as they pertain to SIMS, including the low-flux experiment known as static SIMS.<sup>10</sup> The liquid

**TABLE I. Experimental Characteristics of SIMS**

analyzer types:	quadrupole, sector(s), time-of-flight
mass range:	usually below 2000 dalton; >20 000 dalton possible
vacuum requirements:	$10^{-10}$ Torr for atomic SIMS of clean surfaces; $<10^{-5}$ Torr for molecular SIMS
primary ion current density	
static SIMS:	low current densities, $<1 \times 10^{-8}$ A $\text{cm}^{-2}$ ( $6.3 \times 10^{10}$ ions $\text{s}^{-1} \text{cm}^{-2}$ ); liquid matrices can take much higher currents
dynamic SIMS:	high current densities, usually $>10^{-6}$ A $\text{cm}^{-2}$ ( $6.3 \times 10^{12}$ ions $\text{s}^{-1} \text{cm}^{-2}$ )
primary ion energy:	100–10 000 eV; can use up to 100 keV
primary ions:	Ar <sup>+</sup> , Xe <sup>+</sup> , Cs <sup>+</sup> , O <sub>2</sub> <sup>+</sup> , O <sup>-</sup> , metal ions (Ga <sup>+</sup> , In <sup>+</sup> , Bi <sup>+</sup> , Au <sup>+</sup> , etc.)
primary beam focusing:	100-nm-diameter spot size achievable with liquid metal ion source; 50 $\mu\text{m}$ –1-mm diameter typical for gas sources
sample type:	thin foils; bulk solids; compressed pellets; frozen and liquid matrices (glycerol, thioglycerol, poly(ethylene glycol), triethanolamine, and dithiothritol/dithioerythritol mixtures). Charge compensation often needed for nonconductors.

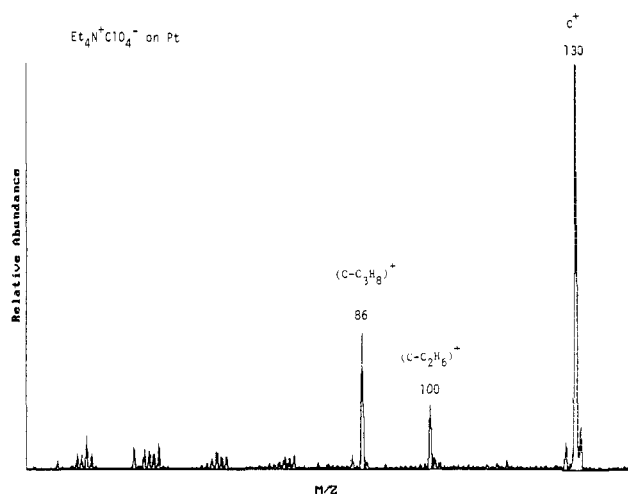


**Figure 1.** SIMS spectrum of a bulk sample of tetraethylammonium perchlorate supported on platinum. Ar<sup>+</sup> bombardment,  $3.4 \times 10^{-11}$  A, 2  $\text{mm}^2$  spot size, 4-keV energy.

SIMS techniques in which high-flux ion beams are used to bombard solution samples are discussed as part of the FAB technique. A recent monograph describes the techniques of SIMS in great detail.<sup>11</sup> Busch<sup>12</sup> has provided an excellent summary of the experimental aspects of SIMS and of the other desorption ionization techniques.

#### 2. Spectral Characteristics of Molecular SIMS

The SIMS mechanism can be obscured by the numerous ion types observed and the variety of systems encountered in the literature. One must recognize, for example, that a monolayer of CO on Ni{001} is a very different system than a thick coating of sucrose on silver. Similarly, peptides supported on solid foils comprise a different type of sample than peptides dissolved in glycerol.

It is generally accepted<sup>13,14</sup> that three distinct types of molecular ions can be produced by particle or photon bombardment of molecules at interfaces: (1) ions resulting from direct desorption of precharged compounds (salts), (2) even-electron ions formed by cationization or anionization viz., clustering of the analyte with available inorganic ions, and (3) radical cations or anions. Each of these ion types will be considered in turn, using Figures 1 and 2 as a basis for discussion. In ad-

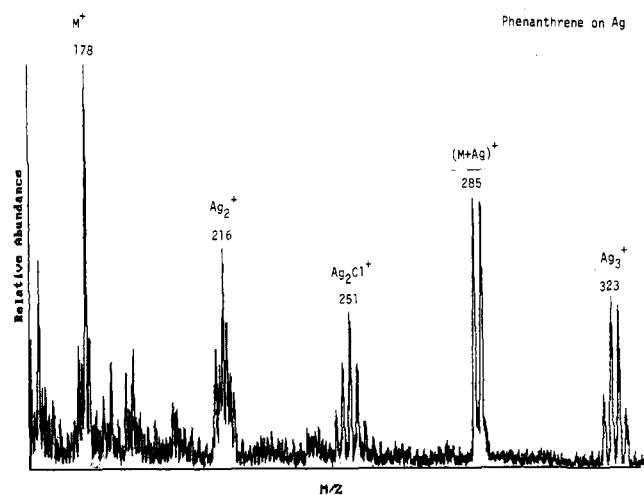


**Figure 2.** SIMS spectrum of a bulk sample of phenanthrene supported on silver foil. Ar<sup>+</sup> bombardment,  $5 \times 10^{-10}$  A, 2 mm<sup>2</sup> spot size, 4-keV energy.

dition to these processes leading to various forms of the molecular ion, fragment ions are also generated. It should be kept in mind that, depending on the nature of the sample matrix and substrate, atomic processes like metal-ion emission can occur, too. Indeed, cationization by a metal ((2), above) is often a consequence of this.

In both molecular and atomic SIMS, precharged materials can be very efficiently desorbed. A simple explanation is that energy is needed only for desorption and not for an additional energy-consuming ionization step. Hence, an organic salt like tetraethylammonium perchlorate gives an unusually abundant signal due to the intact tetraethylammonium cation (C<sup>+</sup>,  $m/z$  130) in its positive SIMS spectrum (Figure 1). The ability of quaternary ammonium salts to give intense ions in SIMS has been known for some time,<sup>15</sup> and picogram quantities of these compounds were used early on to demonstrate the great sensitivity of molecular SIMS.<sup>16</sup> It is interesting that even under mild bombardment conditions (ca.  $2 \times 10^{-9}$  A cm<sup>-2</sup>) the above cation fragments (Figure 1) to give two abundant fragment ions corresponding to formal losses of ethane and propane. Fragmentation processes will be explored further below.

The second type of ion encountered in molecular SIMS is that produced by cation or anion attachment.<sup>17-21</sup> Such an ion appears at  $m/z$  285, 287 in the SIMS spectrum of phenanthrene supported on Ag (Figure 2). This ion corresponds to (M + Ag)<sup>+</sup>, where M is neutral phenanthrene. The usual explanation for formation of this type of ion is that ion-molecule reactions occur in or just above the disordered, high-pressure seldge region produced by sputtering.<sup>13</sup> The adduct (M + Ag)<sup>+</sup> is formed by reaction of sputtered Ag<sup>+</sup> and neutral phenanthrene. The presence of abundant silver cluster ions in Figure 2 supports such an interpretation. In cases where metal-metal bonds are weaker than metal-molecule bonds, however, intact adduct emission from surfaces has been postulated,<sup>22</sup> these situations will be considered later. Metal attachment is just one of the processes that falls into the cationization/anionization category. Ions of the (M + H)<sup>+</sup> and (M - H)<sup>-</sup> type are common in molecular SIMS and other DI techniques, particularly when molecules with polar functional groups are analyzed.<sup>16,17,20</sup> Indeed,

it is now common to manipulate the sample so as to generate precharged ions *in situ*<sup>23</sup> rather than rely on their formation by ion/molecule reactions.

Generation of odd-electron molecular ions in SIMS is relatively uncommon and is usually observed only for compounds known to exhibit great stability as radical ions. The polycyclic aromatic hydrocarbons (PAH) are one such class of compounds, and hence their SIMS spectra<sup>24</sup> are dominated by M<sup>•+</sup> ions. To illustrate, the base peak in the phenanthrene spectrum (Figure 2) is due to the molecular ion at  $m/z$  178. FAB spectra of PAH also give intense M<sup>•+</sup> ions.<sup>25</sup> The origin of odd-electron ions in SIMS has received little study; possible contributing processes include ionization upon collision with massive particles, charge exchange in the seldge, and electron exchange concurrently with desorption. The recent use of electrochemical methods to generate surface species that are analyzed by SIMS<sup>26</sup> should increase interest in these ions. Negative ion SIMS spectra of certain weakly acidic aromatic compounds, such as 1,5-dihydroxynaphthalene,<sup>27</sup> sometimes give abundant M<sup>-</sup> ions. A process which may be analogous, the reduction of positive doubly charged organic ions to give singly charged products, has been well characterized.<sup>28</sup>

Most SIMS spectra contain features due to *fragmentation*. Figure 1, for example, contains fragment ions of a quaternary ammonium salt, and fragmentation can be observed in spectra in which any of the three molecular ion types are formed. The description of fragmentation represents one of the more controversial mechanistic points in molecular SIMS. There are indications that both unimolecular dissociation of molecular ions in the free vacuum and direct decomposition of molecules at the sputtering site can occur. The mechanism of fragmentation will be considered further in section IV.

## B. Fast Atom Bombardment and Other Desorption Ionization Methods

The FABMS technique<sup>29,30</sup> differs from molecular SIMS in two notable ways. Rather than using a charged primary beam, FAB experiments employ neutral beams having translational energies comparable to those used in SIMS. The second feature—probably the more significant from an analytical and mechanistic point of view—is that most FAB (and increasingly, many SIMS) experiments are performed with the analyte dissolved or suspended in a liquid matrix. This minimizes but does not preclude analyte modification (sample damage) and delivers a constant supply of analyte to the interface for analysis. Because neutral primary beams are employed, FAB guns are easily adapted to high-voltage ion sources. On the other hand, the charged primary beam in SIMS allows for better focusing and easy rastering of the beam for secondary ion imaging and depth profiling.

Plasma desorption mass spectrometry (PDMS), the third particle bombardment method to be considered, differs from SIMS and FAB in notable ways, yet certain aspects of the ionization process in PDMS are useful in discussing the SIMS mechanism. The original experimental method—discovered in 1973 by Macfarlane in the course of studies of short-lived radioactive nuclides<sup>31</sup>—involves bombardment of thin films (<10

$\mu\text{m}$ ) with heavy ions of MeV energy produced by spontaneous fission of  $^{252}\text{Cf}$ .<sup>32</sup> Unlike SIMS and FAB, the primary particles perforate the film, and secondary ions are desorbed from both surfaces.  $^{252}\text{Cf}$ -PDMS was the first method to ionize insulin intact,<sup>33</sup> and in fact it gave impetus to the development of SIMS as a method for the analysis of biomolecules.<sup>17</sup> Heavy ions of MeV energy produced in accelerators are also used as projectiles.<sup>34-36</sup> PDMS is very successful at ionizing very large molecules, a process that appears to require very large energy depositions.

The final desorption ionization technique to be dealt with is laser desorption.<sup>37</sup> Often, short (<10 ns) laser pulses of high power ( $10^8 \text{ W cm}^{-2}$ ) are used to generate ions from surfaces. While this method was pioneered in 1963<sup>38</sup> and LDMS of organic salts was reported in the early 1970s,<sup>39</sup> the technique did not begin to enter the mainstream of analytical chemistry until 1978, when LD spectra of large biomolecules were reported.<sup>40</sup> Despite the different method of energy deposition, LD spectra frequently resemble those obtained by particle bombardment. This has implications for the mechanism(s) operating in particle bombardment and justifies the consideration of a seemingly unrelated technique in this paper.

In experiments using laser desorption, and to a lesser extent other DI techniques, increasing attention is being given to separation of the desorption and ionization events. The fact that far more neutrals than ions are typically desorbed recommends this approach as a method of increasing signal. Postionization by photoionization or multiphoton ionization,<sup>41</sup> by chemical ionization,<sup>42</sup> and by electron impact<sup>43</sup> have all been investigated.

Mention should also be made of additional techniques that, while not based on particle bombardment, give spectra somewhat similar to those obtained with the four techniques described above. In field desorption (FD),<sup>44</sup> a kilovolt potential is applied to a filament coated with analyte. The filament is heated to several hundred degrees, and the strong electric field assists in ion emission. A similar technique, electrohydrodynamic (EHD) ionization,<sup>45</sup> uses an electrolyte solution, rather than a filament, as the emitter. Rapid heating of sample placed directly on a filament in the presence of a chemical ionization reagent<sup>46</sup> is effective at producing ions from some involatile and thermally unstable compounds. The thermospray method of introducing LC effluent into a mass spectrometer also produces spectra that show similarities to those obtained in the desorption techniques.<sup>47,48</sup> In thermospray, solvent carrying the analyte is heated and converted into a jet of vapor as it approaches the mass spectrometer ion source. Desolvation ultimately leads to the formation of free gas-phase ions.

### III. Mechanistic Aspects of Atomic SIMS

#### A. Overview

Atomic SIMS represents a useful starting point for discussing the molecular SIMS mechanism, since it provides a vocabulary and a theoretical foundation on which to build. Understanding of the atomic SIMS mechanism has (arguably) reached a higher level than has understanding of the molecular SIMS mechanism.

Reasonable quantitative descriptions of atomic SIMS can be built up by starting from binary collision models. In considering mechanisms in SIMS, it is necessary to deal with both the removal of material from a surface and the ionization of that material.

Some important distinctions must be made at this point. The term sputtering yield refers to the ratio of sputtered *particles* (ions, atoms, and molecules) to primary particles. Secondary ion yield is the ratio of secondary *ions* to primary particles. The term atomic SIMS will mean primarily the analysis of metals, semiconductors, and simple inorganic salts by high primary ion current sputtering ("dynamic" conditions). Low primary ion currents employed in analyses of these materials must also qualify as atomic SIMS, however. Molecular SIMS will mean exclusively the analysis of molecules, usually, but not always, by low primary ion current sputtering ("static" conditions<sup>10</sup>). High fluxes are used in FAB and liquid SIMS, of course. There must, unfortunately, be some ambiguity in terms in such instances as the sputtering of adsorbed gases at metal surfaces. The reality of the situation is that a sharp distinction between atomic and molecular SIMS does not exist, but it is common practice to employ separate terminology.

It may well be that spectral features observed in both atomic and molecular SIMS arise from a combination of "mechanisms". Often one model will explain a certain experimental result while apparently contradicting another. In atomic SIMS, numerous observations have been made that lend insight into the mechanism, and the following list, while not exhaustive, suggests the scope of the problem: (1) Different materials have different sputtering yields.<sup>49-52</sup> (2) Different crystalline forms of the same material may differ in their sputtering yields.<sup>53-55</sup> (3) Sputtering yields depend on the masses and kinetic energies of primary ions.<sup>52,56-58</sup> The primary ion threshold energy for elemental sputtering is ca. 10-30 eV, depending on the material.<sup>57</sup> (4) The incident angle of the projectile affects the sputtering yield.<sup>52,55,59,60</sup> (5) For single-crystal substrates, secondary ions are emitted with a preferred angular distribution.<sup>53,55,61</sup> (6) Sputtered atomic ions have kinetic energies in the electronvolt regime (1-10 eV on average, but with a high-energy tail in the distribution), and these energies increase weakly with primary ion energy.<sup>5,62-65</sup> (7) Secondary ion emission can be enhanced by varying the chemical nature of the analyte. For example, positive ion yields of some metals are enhanced when oxygen is introduced into the vacuum system<sup>66</sup> or implanted in the analyte.<sup>67</sup> Alternatively, sputtering with primary ions of oxygen or other electronegative elements enhances ion yields (especially positive ion yields), while sputtering with electropositive elements such as Cs enhances negative ion yields.<sup>50,68</sup> (8) For positive ions, ionization probabilities depend in an inverse exponential fashion on the ionization energy of the atom. Ionization probabilities for negatively charged ions seem to depend exponentially on the electron affinity of the atom (greater electron affinity results in greater ion yields).<sup>69-71</sup> (9) Precharged materials (salts) produce abundant secondary ions of both polarities.<sup>9,22</sup> (10) Atomic SIMS spectra often show cluster ions composed of several atoms (e.g.,  $\text{Ag}_2^+$ ,  $\text{Ag}_3^+$ ; compare Figure 2).<sup>5,9,72</sup>

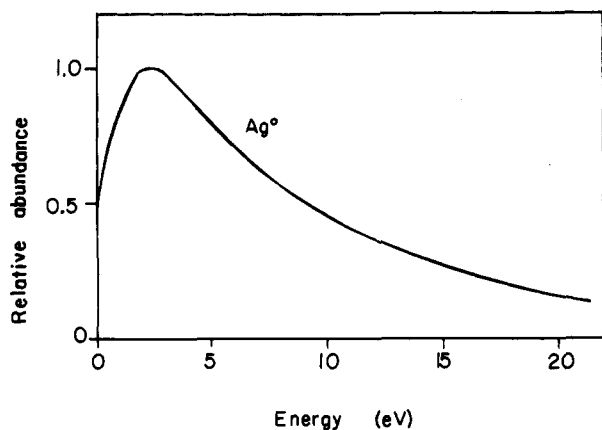


Figure 3. Kinetic energy distribution of Ag atoms sputtered by bombarding silver using 1-keV  $\text{Ar}^+$  ions (from ref 80).

The list above presents a small number of experimental observations that relate to the atomic SIMS mechanism. A number of reviews deal with the subject of atomic SIMS and sputtering at greater length and provide a larger number of references. These include the reviews of Oechsner,<sup>73</sup> McCracken,<sup>74</sup> Winters,<sup>75</sup> Blaise and Nourtier,<sup>76</sup> Williams,<sup>77</sup> Werner,<sup>78</sup> and Greene<sup>79</sup> and the monograph of Benninghoven, Rüdener, and Werner.<sup>11</sup> This paper is concerned primarily with molecular SIMS and therefore deals with atomic SIMS only in enough depth to facilitate the discussion of molecular particle emission/ionization processes.

## B. Sputtering Models

A typical plot of sputtered atom intensity vs. sputtered atom kinetic energy is presented in Figure 3.<sup>80</sup> The particular energy distribution illustrated was obtained by bombarding Ag with 1-keV  $\text{Ar}^+$  at normal incidence, postionizing in a plasma the material ejected perpendicularly, and using a retarding potential for energy analysis. The distribution clearly extends from 0 eV to beyond 20 eV, with the bulk of the atoms having energies in the 1–10-eV range. Energy distributions of this type provide useful indications regarding the processes leading to sputtering.

A small fraction of the sputtered atoms have energies in the thermal regime, below 1 eV. A mechanism whereby local heating by ion bombardment causes evaporation of material is one explanation for the presence of these low-energy atoms. A formal model—the *thermal spike model*<sup>81,82</sup>—has been proposed for this situation. In simple terms, bombardment of a material induces elastic collisions between atoms in the solid, and this collisionally excited region (the “spike”) behaves much like a dense gas at high temperature. Emission of particles occurs by evaporation from the surface of the spike. This model may not be important in atomic SIMS but it is very useful in molecular SIMS (see IVc) where it explains processes which occur late in the desorption event.

At the opposite end of the energy distribution is a high-energy tail that for sputtered ions, falls approximately as  $E^{-n}$ , where  $E$  is the secondary ion kinetic energy and  $n$  lies in the range 1–2.5 for most elements.<sup>64</sup> Atoms with energies of hundreds of electronvolts can be emitted by a *direct recoil* process.<sup>83–85</sup> This involves ejection of high-energy-recoil particles produced by direct momentum transfer from primary ions. In a

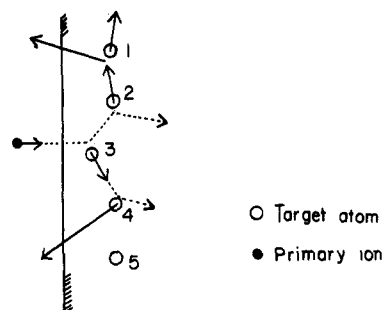


Figure 4. Collision sequences that lead to sputtering of atoms 2 and 4 upon collision of a high-energy particle (●) according to the collision cascade model of sputtering.

typical case, a keV primary ion hits a target atom, transferring a kinetic energy of hundreds of electronvolts to the atom. The atom will be displaced from its position in the lattice, and, if its velocity carries it in an appropriate direction, it will collide with at most a few other atoms before leaving the surface.

The thermal spike and direct recoil models explain the emission of low-energy and high-energy particles, but they are less successful in explaining the emission of the vast majority of particles with translational energies in the 1–20-eV range. The most widely accepted explanation for this behavior is linear cascade sputtering, commonly presented as the *collision cascade model*.<sup>86–88</sup> Sigmund's formulation of this model<sup>87,88</sup> has received wide currency, primarily because it provides a quantitative basis for many of the observations listed above. However, it is still the subject of intense debate and its restriction to binary collisions is thought by some to be an over-simplification.

Like the direct-recoil model, the collision cascade model involves momentum-transfer processes. Figure 4 illustrates the basic principle. Qualitatively, a primary ion of keV energy enters a surface and gradually slows down as it strikes surface and subsurface atoms until it has lost its excess kinetic energy. The various collisions displace target atoms, as well as alter the initially linear trajectory of the primary ion. Recoiling target atoms can strike other atoms, and the so-called collision cascade proceeds until the impact energy is dissipated in a volume of the surface radiating outward from the point of impact. In the course of the cascade, some atoms may acquire momentum in a direction toward the surface and, if the energy of such an atom is greater than the surface-binding energy, the atom will be emitted from the surface. The time scale of a typical sputtering event is extremely short; calculations indicate that atoms are ejected less than  $10^{-12}$  s after the primary ion impact.<sup>89</sup> (This is not to say that later in time processes other than binary elastic collisions do not contribute to ion emission.)

Sigmund's calculations assume random elastic collisions in amorphous and polycrystalline targets composed of only a single element. Transport theory is used to derive a general expression for the sputtering yield in the usual primary ion energy regime (i.e., considerably above the sputtering threshold). This expression is

$$S(x, E, \eta) = \frac{3F(x, E, \eta)}{4\pi^2 N C_0 U_0} \quad (1)$$

where  $S(x, E, \eta)$  is the sputtering yield for primary ions

of energy  $E$  at a surface plane  $x$  and  $\eta = \cos \theta$ ,  $\theta$  being the cosine of the angle of incidence (with respect to the normal) of the primary ion.  $N$  is the density of target atoms,  $C_0$  is a constant related to the cross section for elastic scattering, and  $U_0$  is the surface-binding energy.  $F(x, E, \eta)$  is a function representing the distribution of deposited energy in the lattice; this function is dependent on experimental conditions. For heavy- and medium-mass primary ions of keV energy at perpendicular incidence, the sputtering yield  $S(E)$  is given by the equation

$$S(E) = 0.0420\alpha S_n(E)/U_0 \text{ \AA}^{-2} \quad (2)$$

where

$$S_n(E) = 4\pi Z_1 Z_2 e^2 a_{12} [M_1/(M_1 + M_2)] s_n(\epsilon) \quad (3)$$

$$\epsilon = \frac{M_2 E / (M_1 + M_2)}{Z_1 Z_2 e^2 / a_{12}} \quad (4)$$

$$a_{12} = 0.8853 a_0 (Z_1^{2/3} + Z_2^{2/3})^{-1/2} \quad (5)$$

$M_1$  and  $M_2$  are the masses of the primary ion and target atom, respectively, and  $Z_1$  and  $Z_2$  are the respective atomic numbers.  $\alpha$  is a measure of the momentum-transfer efficiency and is obtained graphically;  $\alpha$  increases gradually with the ratio  $M_2/M_1$ .  $e$  is the electron charge;  $s_n(\epsilon)$  is the reduced nuclear stopping cross section for Thomas-Fermi interactions, obtained by calculating the reduced energy  $\epsilon$  ( $s_n(\epsilon)$  has a maximum for  $\epsilon = \text{ca. } 0.4$ ); and  $a_0$  is the Bohr radius.

The collision cascade sputtering model gives a good match with experimental results under typical experimental conditions.<sup>74,90</sup> The theory is less accurate for very light primary ions because  $\alpha$  becomes too large and for primary ion energies that are either very low (tens of electronvolts) or very high (hundreds of kiloelectronvolts) because the transport theory breaks down. From the equations, several experimental results can be explained. Surfaces with high binding energies will be more difficult to sputter than those with low binding energies; thus, for the elements, sputtering yields correlate inversely with sublimation energies.<sup>57</sup> Sputtering yields will be maximized for a particular primary ion energy and for a particular primary ion-target atom combination. The charge on the primary particle is not important; as long as the momenta of two differently charged, but otherwise identical, particles are the same, there is no reason to expect differences in the collision cascades initiated by the particles.

The Sigmund theory, in addition to predicting yields as a function of target, projectile, and projectile energy, can approximate yields based on the angle of primary ion incidence. For the typical case of backsputtering by ions of moderate mass, incident at angles not too far from perpendicular, the following expression can be applied:

$$\frac{S(E, \theta)}{S(E, 1)} = \eta^{-f} = (\cos \theta)^{-f} \quad (6)$$

$S(E, \theta)/S(E, 1)$  is the ratio of the sputtering yield at incident angle  $\theta$  to that at perpendicular incidence ( $\theta = 0^\circ$  for perpendicular incidence). The constant  $f$  is a function of the mass ratio between the target and projectile. For  $M_2/M_1 < 1$ ,  $f$  is about 1.7; for  $M_2 > M_1$ ,  $f$

slowly decreases to a value slightly less than 1. From the equation, sputtering yields should increase as the incident angle becomes less perpendicular. Equation 6 matches experimental results quite well<sup>91</sup> but is accurate only for  $\theta = 0^\circ$  to about  $70^\circ$ .<sup>75</sup> At oblique angles, experimental yields fall off, probably due to elastic scattering of the primary ions.

## C. Ionization

### 1. Qualitative Models

The Sigmund theory provides a quantitative description of sputtering. It is limited, however, to single-element, amorphous or polycrystalline targets and predicts atomic sputtering yields, not secondary ion yields. Where ion emission from multielement surfaces is concerned, quantitative theories are virtually nonexistent. The usual approach is to qualitatively describe the factors that affect secondary ion yields so as to provide a basis for predicting experimental results.

It is well-known that both neutrals and ions are produced by sputtering and that, with few exceptions (e.g., salts and some oxides) the ionic component is small. Ions are of more interest, however, because they are easily detected. In addition to being low, ion yields are highly susceptible to matrix effects, making accurate quantitation difficult. For these reasons, methods have been developed for production of ions from sputtered neutrals,<sup>41-43,92-95</sup> neutral yields being immune to many of the factors that influence secondary ion yields. Nevertheless, SIMS continues to dominate as a practical technique, and the mechanism of ionization remains an important subject. Williams<sup>77</sup> has provided a valuable summary and critical evaluation of the principal ion formation models that have been advanced. The following presentation draws heavily from his work, but it also considers more recent data.

For ions to be ejected from a surface, it is necessary that electron-transfer processes occur (except in the case of precharged compounds; see below). The electronic structure of the surface during sputtering must therefore have a profound effect on secondary ion yields. There are a number of factors that can influence the surface electronic structure, including the presence of reactive gases like oxygen and the degree of disorder generated by the collision cascade. A collision cascade in a lattice will involve a significant number of non-glancing, or "hard", collisions. Such hard collisions can provide enough energy to reduce the normal crystal spacing between collision partners; the atoms will be driven up the repulsive portion of the potential energy curve. This process may result in an electron of given energy crossing from one atom to a different electron energy level in another atom. Such a process can lead to ionization which may also be accompanied by electronic excitation. Thus electronic excitation is possible in a collision cascade, and this may itself lead to ionization, for example, in the form of autoionization, Auger processes, or direct electron emission into the continuum.<sup>77</sup> Inelastic processes of this type can take up a good fraction of the energy of a recoil; a 254-eV <sup>73</sup>Ge recoil in Ge loses about 39 eV to ionization,<sup>96</sup> corresponding to 15% of the total. The experimentally observed ion kinetic energy distribution may depend on both collisional excitation and on deexcitation processes which

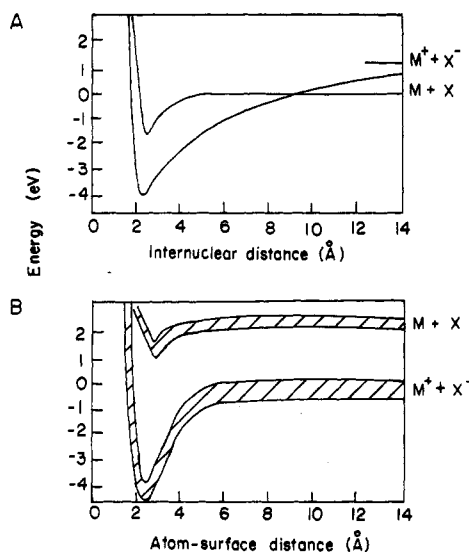


Figure 5. Gas-phase (A) and condensed-phase (B) potential energy surfaces for ionic compounds MX.

occur as a sputtered atom or ion leaves the surface.

In the case of simple ionic compounds, the *bond-breaking model* is often invoked to explain ion emission.<sup>97,98</sup> A typical lattice—that of NaCl, for example<sup>77</sup>—will contain a valence band of anionic states and a conduction band of cationic states, separated by a band gap<sup>99</sup> (ca. 10 eV for NaCl). Removal of a sodium ion from NaCl requires half the lattice energy, since only half the lattice is made up of  $Na^+$ . The NaCl lattice energy is about 8 eV, so 4 eV will be necessary for  $Na^+$  to escape. For emission of *neutral* sodium, an electron must cross the 10-eV band gap, and the atom would have to undergo a transition from the condensed phase to the gas phase. At the surface, both the lattice energy and the band gap are diminished by roughly half. This leaves a 3-eV difference favoring ion emission over neutral emission, and hence ion emission dominates. The same argument should apply to emission of  $Cl^-$ . Another way to explain the bond-breaking model for salts is that, in contrast to the gas phase (see Figure 5A), potential energy curves for ionic and covalent interactions near a solid surface (ion and neutral emission, respectively) do not cross, except in the repulsive region (see Figure 5B). If high-energy collisions drive the system up the repulsive portion of the curve, crossing to the neutral curve becomes possible. This model can also be used to explain ion emission from covalent compounds. As long as there is some polar character, a band gap will exist, and ion emission will be favored if the lattice energy is much less than this band gap. It may be argued, then, that formation of a metal oxide (for example, by adsorption of residual oxygen) will cause emission of a greater ratio of ions-to-neutrals than would be the case without the oxide-induced band gap.

Discussion of atomic ion emission by sputtering almost invariably deals with matrix effects, such as oxygen enhancement of ion yields, since these effects are of considerable magnitude. While the bond-breaking model is appealing, it applies mainly to polar materials, and it fails to explain the enhanced emission of *negative* ions<sup>100</sup> from oxygenated surfaces. Williams<sup>101</sup> has questioned the validity of assuming that an ionic solid is an assembly of discrete ions, since the electron den-

sity distribution of such a material is identical with that of an assembly of neutral atoms. Emission of an ion like  $Si^-$  from  $SiO_2$  could be explained by the creation of "anti-site defects". If a silicon atom were collisionally forced into an oxygen site, it would tend to behave on ejection like oxygen and would be emitted as  $Si^-$ . This model and the conventional bond-breaking model both imply that ions are emitted directly from the surface. Gnaser,<sup>98</sup> however, found evidence for gas-phase dissociation of M-O molecules sputtered as intact units. A plot of  $M^+$  vs.  $O^-$  intensities for pure metals under oxygen was linear, with a slope of 1, indicating that  $M^+$  and  $O^-$  may be formed in the same mechanistic step—possibly via dissociation of M-O. If the sputtered molecule has sufficient energy to dissociate, ion formation may occur by level crossing in the "rebound" step after the system has been pushed up the repulsive portion of the potential energy curve. This model is essentially the *molecular model* proposed by Thomas.<sup>102</sup> The model is most applicable to sputtering of oxides and does not explain sputtering of salts like NaCl as well as does the bond-breaking model.

Sputtering with primary ions such as  $O_2^+$ ,  $O^-$ , or  $Cs^+$  derived from reactive gases has been employed for a number of years as a means for optimizing yields and obtaining consistent, reproducible data.<sup>68</sup> The usual explanation of this effect is that primary species are implanted in the substrate, where they act as they would in the case of reactive gas adsorption. A simple but incomplete explanation of oxygen enhancement is that oxygen acts to increase the work function of a surface, making it more difficult for thermionic electrons to neutralize gas-phase ions. This explanation has several flaws, not least of which is the fact that *decreasing* the work function can enhance positive ion yields<sup>103</sup> (although the macroscopic work function is not necessarily the same as that at the disordered sputtering site). In addition, thermionic electrons are not usually observed, and, if they were present, there is a low probability that they would neutralize ions anyway, since the probability for radiative attachment is extremely low.<sup>77</sup>

Another model, the *band structure model*,<sup>22,104,105</sup> is somewhat more successful and predicts oxygen enhancement of both positive and negative ion yields. This model assumes that the band structure of a solid influences electron transfer between excited atoms or ions and the solid. For a pure metal surface, there is a good chance that sputtered ions will undergo neutralization by electron transfer to or from the conduction band of the metal. For oxides, however, neutralization is less likely, because there will no longer be electrons available in the conduction band for transfer and the energies of electrons in the valence band will be too low for resonant exchange with higher energy excited atoms or ions. In the band structure model, positive ion enhancement is viewed as the result of the absence of electron transfer to departing positive ions, while negative ion enhancement is due to electron attachment to departing neutrals. This attachment can occur if excited electrons are thermalized in the high-energy oxide conduction band.<sup>77</sup> While the band structure model gives a reasonable explanation of yield enhancement effects, it suffers from several difficulties. Because the sputtering region is undoubtedly highly

disordered, it is questionable whether a bulk band gap model (or a bulk work function model) is applicable;<sup>77</sup> experimental evidence of this disorder lies in the observation that mixing of atoms in the collision cascade is one of the primary resolution-limiting factors in depth profiling.<sup>106</sup> Furthermore, semilog plots of elemental ion yields from oxide matrices vs. pure element ionization potentials are linear over a wide range,<sup>107</sup> even though large increases in ion yield would be expected as ionization potentials move past the maximum valence band energy.

In an attempt to further refine the various ion emission models, Williams and Evans<sup>100</sup> introduced the *surface polarization model*. An attractive feature of this model is that it deals with the actual microscopic area from which sputtering occurs, rather than with the bulk material. Oxygen is thought to enhance positive ion yields when absorbed at the surface and to enhance negative ion yields when incorporated into the substrate. Since virtually all substrates in SIMS are less electronegative than oxygen, local surface dipoles can be created. For surface oxygen the high electron density on oxygen will create a potential barrier for electrons that could otherwise neutralize positive ions. This barrier will be absent when oxygen is below the surface. The probability that neutralization will occur is thus determined by the surface-oxygen dipole orientation. An experiment<sup>100</sup> in which Si was sputtered by argon, initially under a flow of oxygen and later with the flow turned off, shows that Si<sup>+</sup> yields decrease as adsorbed oxygen is sputtered away, while Si<sup>-</sup> yields simultaneously increase. After a length of time corresponding to removal of adsorbed oxygen, both negative and positive ion yields gradually fall, although the Si<sup>-</sup> yield remains much higher than the Si<sup>+</sup> yield. This slow falloff correlates with removal of oxygen recoil-implanted during the early stages of the sputtering process.

## 2. Semiquantitative Models

The models described to this point illustrate the difficulty of explaining the ionization processes. The models are qualitative, and they have been applied in depth only to very specific situations, e.g., oxygen enhancement of metal ion yields. These special situations are sometimes the easiest to explain. The bond-breaking model, for example, is a good explanation for ion emission from salts like NaCl. For sputtering of pure elements, on the other hand, the above models are less applicable. The band structure model explains the low ion-to-neutral ratios from metals, but not the fact that some ions are not neutralized. A model whereby secondary electrons ionize sputtered neutrals<sup>108</sup> also seems unlikely to be of great importance.<sup>77</sup> Intuitively, since secondary electrons arise in the first few surface layers and since electron velocities are much higher than atomic velocities, the vast majority of secondary electrons will be gone before atoms even begin to leave the surface.

In a sense, the models described to this point are all very similar. *Ions either preexist in the solid or are formed by electronic excitation in the collision cascade, and the observed ion distribution is mediated by electron-transfer processes.* This is not the only possible scenario, however. A common approach for treating ionization, particularly in the community

concerned with quantitative analysis by SIMS, is to consider the sputtering region to be a "dense plasma in local thermal equilibrium".<sup>69</sup> This assumption is probably invalid, because, among other things,<sup>77</sup> calculations<sup>54</sup> indicate that the number of collisions necessary for particle ejection is far lower than the number needed for equilibration. This *local thermal equilibrium (LTE) model*, however, accounts for the approximate dependence of ion yields on ionization potentials and electron affinities. When thermal equilibrium is assumed, the Saha-Eggert ionization equations can be used to predict the ratio of positive or negative ions to atoms as follows:

$$K_{n^+} = \left( \frac{2\pi}{h^2} \frac{m_{N^+} m_{e^-}}{m_{N^0}} kT \right)^{3/2} \frac{B_{N^+} B_{e^-}}{B_{N^0}} \exp(-I/kT) \quad (7)$$

$$K_{n^-} = \left( \frac{2\pi}{h^2} \frac{m_{N^0} m_{e^-}}{m_{N^-}} kT \right)^{3/2} \frac{g_{N^0} g_{e^-}}{g_{N^-}} \exp(A/kT) \quad (8)$$

$K_{n^+}$  is the dissociation constant for the equilibrium reaction in which a neutral atom  $N^0$  dissociates to the ion  $N^+$  and an electron  $e^-$ , while  $K_{n^-}$  is the dissociation constant for the equilibrium reaction in which a negative ion  $N^-$  dissociates to a neutral atom  $N^0$  and an electron  $e^-$ ,  $h$  is Planck's constant,  $m$  is the mass of a given particle,  $k$  is Boltzmann's constant, and  $T$  is the absolute temperature in the plasma.  $B$  and  $g$  are partition functions,  $I$  is the first ionization potential of the atom, and  $A$  is the electron affinity of the atom. Andersen and Hinthorne<sup>69</sup> applied this model rather successfully to convert experimental ion intensities into quantitative elemental analyses.

The LTE model, despite its possibly erroneous basis, does at least give a numerical method for predicting ion yields. This model has led to more sophisticated models which also make use of ionization potential and electron affinity dependences. Nørskov and Lundqvist,<sup>71</sup> considering sputtering of pure metal surfaces, claim that ions generated in a collision cascade will be entirely neutralized as they leave the surface and that the relevant source of excitation is actually the time-varying potential of the sputtered particle as it leaves the surface. At a particular distance from the surface, electronic interactions will not be possible and, if ionization occurs shortly before a sputtered particle reaches this distance,<sup>109</sup> it may survive as an ion. This model has been described as the *electron-tunneling model*<sup>110,111</sup> because ionization is the result of resonant electron transfer between the departing atom and the electron gas of the metal. The following expressions represent the probabilities  $\alpha^{+(-)}(E)$  in the model that sputtered particles will be emitted as ions:<sup>71</sup>

$$\alpha^+(E) = \frac{2}{\pi} \exp[-\pi c_1(I - \phi)/\hbar\gamma v] \exp[-\pi c_2/\hbar\gamma v] \quad (9)$$

$$\alpha^-(E) = \frac{2}{\pi} \exp[-\pi c_1(\phi - A)/\hbar\gamma v] \exp[-\pi c_2/\hbar\gamma v] \quad (10)$$

The constants  $c_1$  and  $c_2$  are related to the varying difference between the ionization potential  $I$ , or the electron affinity  $A$ , and the Fermi energy as a particle moves away from the surface.  $\hbar$  is Planck's constant divided by  $2\pi$ ,  $\phi$  is the work function of the surface,  $\gamma$  is the maximum distance at which electron transfer between the particle and the surface can take place, and



$v$  is the particle velocity component perpendicular to the surface. The equations imply that the velocity (and therefore the kinetic energy) of a sputtered particle affects the probability of its emission as an ion. Higher velocity particles will have a greater ionization probability than those with low velocities. Equation 10 for negative ions is supported by experiments<sup>112</sup> that show an exponential velocity dependence for emission of  $O^-$  from oxygen chemisorbed on V and Nb. Vasile<sup>65</sup> has demonstrated a similar dependence for positive ions ejected from Cr, Ag, Cu, and Zr; these data are complemented by semiempirical molecular orbital calculations for Al.<sup>113</sup>

Recently Yu and Mann<sup>114</sup> described a local bond-breaking model—within the framework of the electron-tunneling model—to account for enhanced yields of  $Si^+$  from oxidized and nitrated surfaces. While the work function is an important quantity in the electron-tunneling model, it is the *localized* substrate electronic state that becomes important in their local bond-breaking model. This model begins to bridge the gap between the qualitative and semiquantitative models of secondary atomic ion emission.

Both Williams<sup>77</sup> and Sroubek<sup>115</sup> have proposed a model subtly different from the electron-tunneling model. Lin and Garrison<sup>116</sup> have considered angular and velocity effects as related to this model, but the model awaits firm experimental confirmation. Blaise and Nourtier<sup>76</sup> and Veksler<sup>117</sup> have reviewed these and other semiquantitative theories in greater depth, particularly as they relate to ion emission from pure metals.

From the overview given here, it becomes apparent that no single description of atomic SIMS can explain all of the experimental results. There appear to be two dominant ionization processes, however. The first results from perturbation of outer atomic electrons in the sputtered particle during its flight from the surface (section III.C.2). The second comes into play for chemically complex systems (e.g., salts and adsorbed reactive gases) and involves electron transfer associated with collisional excitation of the lattice (section III.C.1). Particle emission itself is explained adequately through invoking both the process of sputtering via collision cascades and particle evaporation from material in the quasi-equilibrium state known as the thermal spike. The question of which of these two processes dominates in molecular SIMS is central to much of the discussion in section IV.

#### D. Additional Aspects of Atomic SIMS

The emission of clusters has long been recognized as a feature of atomic SIMS, and it is of particular interest here because of its relation to molecular SIMS. Calculations indicate that simple atomic clusters such as  $Ar_{2-25}$ ,  $Cu_5$ ,  $Cu_3$ , and  $Cu_2$  arise from recombination of sputtered atoms in the near-surface region, rather than by direct emission of intact clusters from the surface.<sup>72,118,119</sup> Atoms that comprise clusters formed by recombination need not have been contiguous in the surface, but do originate from a very small volume. There is experimental evidence<sup>120</sup> that the formation of  $In_2$  and  $In_2^+$  proceeds by similar mechanisms and hence that conclusions based on comparisons between neutral and ionic clusters are probably valid. Some experiments suggest, however, that clusters can emerge

intact, as in sputtering of negative carbon ions from cesiated graphite.<sup>121</sup> The question of cluster emission will be considered more thoroughly in section IV.

The final aspect of atomic SIMS to be discussed is the emission of multiply charged ions. It has been suggested<sup>122</sup> that multiply charged transition-metal ions are formed in the gas phase by impacts of primary ions and sputtered atoms. Alternatively, they can result from core-level ionization followed by Auger decay. Light elements tend to have core-vacancy lifetimes which are long enough for Auger electron emission to occur after the atom has left the surface.<sup>123</sup> The occurrence of multiply charged ions gives some idea of the *internal* energy distribution of ions in SIMS, a little-studied but important quantity that will be dealt with again in connection with molecular analytes. At an  $Ar^+$  primary ion energy of 2 keV, the ratio of  $Al^+$  to  $Al^{2+}$  to  $Al^{3+}$  generated from Al is approximately 2000:200:1.<sup>124</sup> The first, second, and third ionization potentials of Al are 6.0, 18.8, and 28.4 eV, respectively.<sup>125</sup> This implies that the singly charged Al ions have internal energies between 0 and 12.8 eV (12.8 eV is the difference between the first and second ionization potentials); about 90% of the sputtered ions are singly charged and must therefore have internal energies in this range. The other 10% are mainly doubly charged ions with internal energies of 0 to 9.6 eV (i.e., 12.8–22.4 eV above the  $Al^+$  ground state). It should be stressed that these *internal* energies are to be contrasted with the often reported atom or ion *kinetic* energies (such as those plotted in Figure 3) which can extend up to several hundred electronvolts.

### IV. Mechanistic Aspects of Molecular SIMS

#### A. Overview

Although molecular species have long been observed as contaminants in SIMS spectra and as early as 1967 a systematic study of polymers was attempted,<sup>126</sup> molecular SIMS did not evolve until after the development of the static SIMS method.<sup>10</sup> In 1970 Benninghoven published negative ion SIMS spectra of various linear carboxylic acids,<sup>127</sup> but it was not until 1976 (after the emergence of <sup>252</sup>Cf-PDMS) that the potential value of the method was realized by Benninghoven and co-workers<sup>17</sup> and by Winograd, Cooks, and their co-workers.<sup>18</sup>

The key innovation in static SIMS was the use of a low primary ion current density to minimize sample damage. A simple calculation can be performed to see why low currents are necessary. Typical primary ion currents used in atomic SIMS are  $1 \times 10^{-5}$  A  $cm^{-2}$  or more, corresponding to about  $6 \times 10^{13}$  ions  $s^{-1} cm^{-2}$ . Damage cross sections (regions of extensive target atom displacement) due to collision cascades have been calculated to be about 200 Å<sup>2</sup> for 600-eV  $Ar^+$  on Cu.<sup>54</sup> While perhaps not quantitatively applicable to molecular SIMS, such a cross section provides a guide on which a calculation can be based. When an interaction ("damage") area of 200 Å<sup>2</sup> and a primary ion flux of  $6 \times 10^{13}$  ions  $s^{-1} cm^{-2}$  are assumed, this area would undergo a primary ion hit every 0.8 s. Acquiring a SIMS spectrum over even the relatively short period of 1 min would then require sampling of secondary ions arising from areas that had been struck by primary ions as

many as 75 times. This may be acceptable for atoms but, in the case of molecules, which can fragment or react at the surface, it could make analysis impossible. Reducing the ion current to  $1 \times 10^{-8}$  A  $\text{cm}^{-2}$  ( $6 \times 10^{10}$  ions  $\text{s}^{-1}$   $\text{cm}^{-2}$ ), however, gives one hit every 14 min, and another tenfold reduction allows analysis of virgin surface for over 2 h, although secondary ion signals drop correspondingly.

In describing the mechanism of molecular emission in SIMS, a first step might be to attempt to correlate molecular data with the wealth of atomic SIMS theory. There may be similarities between the processes resulting in atom and in molecule emission, but an energetic collision cascade alone would seem an improbable means by which to eject *intact* molecules, particularly large biomolecules. Most of the molecular SIMS models that have been advanced therefore incorporate a thermal component into the mechanism. In what follows, several different views of molecular desorption will be examined, beginning with the models most closely resembling those in atomic SIMS and working toward models focused mainly on molecular processes. In simple terms, the mechanisms of molecular SIMS encountered in section B are based on what may be termed *translational mechanisms* and those of section C can be classed as *thermal* or *vibrational mechanisms*. These terms are used to underscore the principal immediate cause of molecular ejection from the condensed phase. Of course, in a time-dependent and position (with respect to impact site)-variant phenomenon these terms can serve only as very rough labels. It will become apparent that the dominant molecular ion emission process in SIMS can be summarized briefly, if not entirely adequately, as a vibrational desorption process. It will also be apparent that the ionization state (and chemical form) of the ejected particle is largely controlled by the chemical state of the analyte and by ion/molecule reactions occurring in the selvedge.

## B. Collision Cascade Models

### 1. Classical Dynamics Model

The studies of Garrison and Winograd<sup>89</sup> suggest that some aspects of molecular SIMS can be explained by assuming a collision cascade model. This work is based in large part on computer simulations first developed by Harrison.<sup>53,128,129</sup> In a typical calculation, parameters such as primary ion mass, energy, and angle, and the size, depth, and crystal structure of the target are first defined. Classical equations of motion are then applied to compute the position and momentum of each particle as a function of time.<sup>54</sup> The time scale is in femtoseconds ( $1 \text{ fs} = 10^{-15} \text{ s}$ ), with molecular ejection usually occurring in less than 200 fs. This *classical dynamics model* is most successful in predicting sputtering effects on single-crystal surfaces, and it has contributed to the understanding of cluster formation, angular discrimination, and emission and fragmentation of adsorbed organic molecules.

Garrison<sup>130</sup> has described several cluster formation mechanisms in SIMS. One, already mentioned, involves recombination of sputtered atoms in the near-surface region. It applies mainly to metals and atomic adsorbates on solids, but it also operates in some bulk materials like solid argon.<sup>72</sup> This clustering mechanism is

best described as an *atomic* SIMS process. A second process is suggested to be responsible for direct emission of molecules. A simple adsorbate like CO can be sputtered largely intact—in a manner analogous to the sputtering of an atom—because the C–O bond (11.1 eV) is much stronger than the metal–molecule bond (1.3 eV).<sup>131</sup> Isotope-labeling experiments<sup>132</sup> support the contention that CO can be emitted without cleavage of the C–O bond. A large molecule, on the other hand, is unlikely to receive enough energy from a single cascade recoil to cause it to leave the surface. Calculations for benzene adsorbed on Ni{001}, however, indicate that intact ejection *can* be induced by a collision cascade if several parts of the molecule are struck in a concerted manner.<sup>133,134</sup> These calculations are supported by the following facts: (1) Multiple collisions in a solid act to dissipate the high energy of the primary particle. (2) The internal vibrational modes of a molecule can accommodate excess energy from a violent collision. (3) Metal substrate atoms are much larger than carbon atoms, making the probability for concerted hits higher than might be suspected. Garrison<sup>134</sup> suggests that such a “concerted push” might explain the desorption of large biomolecules, since the diameter of a benzene ring is about 5 Å, while the diameter of myoglobin (molecular weight 16900) is less than an order of magnitude larger (35 Å). In addition, while benzene  $\pi$ -bonds to surfaces and thus lies flat, very large molecules that stand (more or less) erect may be unexpectedly easy to eject.

Intact benzene ejection is most likely when the molecule is struck by substrate recoils. If a benzene molecule is hit directly by a primary ion, fragmentation might be expected to occur. SIMS spectra of Ni taken under high benzene coverage show more extensive hydrocarbon fragmentation than spectra taken under low coverage,<sup>135</sup> and this is taken to support the suggested fragmentation mechanism, since high coverage makes possible a greater number of direct primary hits. This is consistent with the observation that frozen benzene displays extensive rearrangement and fragmentation.<sup>136,137</sup> The classical dynamics calculations allow estimates of *internal* energies to be made, and in the case of benzene about 75% of the molecules have energies less than 5 eV, with the median energy being about 2.5 eV.<sup>134</sup> This is below the fragmentation threshold, suggesting that unimolecular dissociation is not a dominant process and that direct fragmentation occurs at the surface (see below). Angle-resolved SIMS experiments<sup>138</sup> for chlorobenzene on Ag are interpreted as showing that the ion  $(\text{C}_6\text{H}_3)^+$  arises from surface fragmentation of  $(\text{C}_6\text{H}_5\text{Cl})^+$  because polar angle distributions for the two ions are similar. The results for benzene itself are somewhat inconclusive but are interpreted as showing that the ions  $(\text{C}_6\text{H}_5)^+$  and  $(\text{C}_4\text{H}_3)^+$ , also, do not arise from gas-phase dissociation of  $(\text{AgC}_6\text{H}_6)^+$ .<sup>132</sup>

The third cluster mechanism described by Garrison<sup>130</sup> is a hybrid of the two already mentioned. Formation of species like  $(\text{NiCO})^+$ ,  $(\text{Ni}_2\text{CO})^+$ ,  $(\text{NiC}_6\text{H}_6)^+$ , and  $(\text{AgC}_6\text{H}_6)^+$  is thought to result from recombination of intact molecules and metal ions in the near-surface region, that is, by the cationization process recognized early in the development of molecular SIMS.<sup>18</sup>  $(\text{NiC}_6\text{H}_6)^+$ , for example,<sup>134</sup> forms by recombination of ejected  $\text{Ni}^+$  and  $\text{C}_6\text{H}_6$ , which need not have been con-

tiguous in the surface. No  $(C_6H_6)^+$  is observed in the SIMS spectrum of benzene on Ni, since the ionization energy of Ni (7.6 eV) is lower than that of benzene (9.2 eV). In addition, the calculations predict that the individual adduct components are near each other after ejection and that their relative velocities are small. An alternative to recombination is intact ejection of a  $(NiC_6H_6)^+$  adduct. This seems unlikely, as it would require breaking several Ni–Ni bonds (0.58 eV each<sup>131</sup>) while retaining a Ni–benzene bond (total binding energy estimated to be about 1.7 eV<sup>134</sup>).

The above description of the clustering process bears similarities to descriptions of ion/molecule reactions occurring in the seldge in models based on vibrational desorption (section IV.C). Useful as it is, more detailed tests will be necessary to help resolve the contributions by the translational (collision cascade) and the thermal desorption processes discussed in section IV.C, below.

The kinetic energy distributions of desorbed organic ions provide experimental data against which SIMS mechanisms can be tested. This information provides substantial support for the collision cascade model in atomic systems. Data<sup>139</sup> available for organic ions show the absence of the high-energy tails characteristic of collision cascades. However, ions that acquire high translational energies are most likely to acquire high internal energies (hence fragmentation will tend to remove the high-energy tail and molecular ions of lower translational energy will survive). This is consistent with data which show that fragment ions have higher kinetic energies than molecular ions.<sup>130</sup> These experimental data do not allow a distinction to be drawn between the collision cascade and vibrational desorption models since the latter might also be expected to give narrow distributions of low average kinetic energy.

The classical dynamics model has a number of obvious advantages and disadvantages. The major advantage is that it allows semiquantitative predictions of actual behavior, including the species ejected and their energy and angular distributions. It is conceptually simple, has a basis in reasonably well-understood atomic sputtering theory, and provides one rationalization for such aspects of molecular SIMS as cationization/anionization and fragmentation. It is primarily a model for sputtering, and not for ionization; parallels must therefore be established between neutral and ion emission. As a tool for studying molecular SIMS, it has been applied mainly to simple, well-defined systems like monolayers of CO or benzene on Ni{001}. The degree of applicability of the model for bulk molecular insulators and biomolecules is not yet clear.

## 2. Precursor Model

The concepts that follow deal chiefly with the mechanism of ionization and secondarily with the momentum-transfer problem. The idea that precharged analyte ions are observed preferentially to ionized forms of the initially neutral analyte is the key to the preformed ion<sup>13</sup> or precursor<sup>140</sup> model. Although presented by Benninghoven in terms of collision cascades, the same ionization concepts have also been used in the context of thermal desorption.

Benninghoven<sup>140</sup> advocates a scheme of graded energy deposition and defines a function,  $\bar{E}(r)$ , to describe the average energy transferred to a surface particle at a

given distance from the impact point. Magee<sup>83</sup> stresses that the area nearest the primary ion impact point will be highly disordered and takes the view that a large part of the sputtered particle emission from this region will be due to direct knock-on processes. For 10-keV  $Ar^+$  at perpendicular incidence on Cu, this area has been calculated to be roughly 20 Å in radius.<sup>141</sup> Any molecules in this high-energy-collision area will undergo extensive fragmentation. At distances of 30–40 Å from the impact point, however, sputtering as a result of a linear cascade mechanism prevails, and the recoil energies should be low enough to permit ejection of intact molecules by a “concerted push” as described by Winograd and Garrison.

Benninghoven, drawing chiefly from results for monolayers of amino acids on clean metal surfaces, describes a *precursor model* for molecular ion emission. This model suggests that before an ion is emitted it exists on the surface in the form of a precharged “precursor”. For the simple case of metal oxide sputtering,<sup>142</sup> metal ions will tend to be emitted as positive ions, while oxygen ions will tend to be emitted as negative ions, reflecting their charge states in the lattice. Metal oxide cluster ions that are rich in metal atoms will bear positive charges, while oxygen-rich clusters will bear negative charges. Clusters are thought to be emitted *intact*, and not by recombination, which clearly differs from the Winograd–Garrison view (note that the systems studied are different, however).

Organic ion emission is also proposed to arise from surface precursors, and the fact that the clean metal substrate can influence the formation of  $(M + H)^+$  and  $(M - H)^-$  ions from amino acid overlayers<sup>143,144</sup> provides support. Ion yields vary by as many as 3 orders of magnitude, depending on the metal. For example, leucine monolayers on Ag, Pt, and Au give very high  $(M + H)^+$  and  $(M - H)^-$  yields, while on other metals (Co, Ni, and Cu) they give only  $(M - H)^-$ . The lack of  $(M + H)^+$  ions for some metals can be explained by strong bonding (chemisorption) between the amino acid and the metal. Emission of  $(M + H)^+$  does not occur because the precursor on the surface is a complex of the form  $[metal^+-(M - H)^-]$ , which favors emission of  $metal^+$  and  $(M - H)^-$ . Yields of  $Cu^+$  and  $(M - H)^-$  increase in parallel as amino acid coverage approaches a monolayer, suggesting that metal–acid adducts either fragment after intact ejection or that  $Cu^+$  and  $(M - H)^-$  are emitted in the same sputtering event. If charged precursors were not formed, it would be difficult to explain why the yield of  $Cu^+$  increases as the Cu substrate is covered. Chemisorption on unreactive (noble) metals such as Au is not expected, and the emission of  $(M + H)^+$  and  $(M - H)^-$  can be explained by proton exchange between adjacent *physisorbed* molecules. Once again, as monolayer coverage is approached, yields of positive and negative ions increase in parallel. Deuterium-labeled amino acids were used to demonstrate that proton exchange occurs between amine groups,<sup>145</sup> although dissociative  $H_2$  adsorption on Pt can also provide protons in the case of submonolayer amino acid coverage.<sup>146,147</sup>

These ideas are further supported by the fact that multilayers of amino acids produce  $(M + H)^+$  and  $(M - H)^-$  ions independently of the identity of the metal substrate. In addition, an acidified glycine solution

gives larger  $(M + H)^+$  yields than do nonacidified solutions,<sup>20</sup> and mixing of *p*-toluenesulfonic acid with biological molecules on surfaces increases  $(M + H)^+$  ion abundances.<sup>23</sup>

Other aspects of the precursor model include the assumption that energy transfer to molecules is assumed to occur very rapidly, resulting in a high probability for unfragmented secondary ion emission. This is one reason why SIMS spectra often resemble spectra obtained by LDMS and PDMS, which also involve fast energy transfer. Fragmentation occurs in some cases and may result from transfer of a large amount of energy near the impact point or from gas-phase decomposition of an excited molecule. Evidence for gas-phase decomposition (unimolecular dissociation) will be considered in more depth in section IV.C. The main aspect of the precursor model is that the charge state of the surface precursor is maintained during desorption. In summary, the precursor model adds to the mechanistic foundation provided by Winograd and Garrison by considering chemically complex systems like amino acids. It focuses on the chemical and charge state of the analyte. Significantly, its validity does not necessarily require the assumption of a collision cascade model, and most of its conclusions can be couched in terms of the thermal models that are now considered.

### C. Thermal and Vibrational Models

Up to this point, models have been presented that explain secondary ion production based largely on collision cascade processes. In this section, detailed attention is given to the work of three groups (those of Rabalais, Michl, and Cooks) who suggest that ion emission may be better described as involving processes occurring under conditions which more closely approach thermal equilibrium.

Rabalais<sup>9,22,137</sup> makes use of the selvedge concept to explain ion emission in molecular SIMS and proposes that the mechanism involves "transient thermal activation of a localized site by a single ion impact followed by irreversible expansion to relieve the nonequilibrium situation".<sup>22</sup> Two important aspects of Rabalais's contributions to SIMS are that they integrate both ejection and ionization and can be applied to many different systems.<sup>22</sup> Emission of ions from metals is explained with a band-gap model, as is emission of ions from insulators like  $\text{SiO}_2$ . For ionic solids the bond-breaking model is used. These are all, of course, standard explanations of atomic SIMS. For molecular SIMS, molecular solids are divided into two subgroups: those with strong *intermolecular* forces and those with weak *intermolecular* forces. The former category is typified by polar molecules in frozen form. The positive SIMS spectrum of frozen  $\text{H}_2\text{O}$ <sup>137</sup> is dominated by clusters of formula  $(\text{H}(\text{H}_2\text{O})_n)^+$ , where  $n = 1$  to at least 51. Kinetic energy distributions of these water clusters show narrower, lower energy peaks with increasing cluster size. Ejection is thought to arise as a result of the very high effective temperatures produced by a collision cascade in the sputtering region. Clusters are formed by recombination in the selvedge. A band structure analysis<sup>22</sup> shows that only  $(\text{H}_3\text{O})^+$  is likely to be emitted without neutralization, suggesting that large cluster ions are formed by interactions of sputtered neutrals with  $(\text{H}_3\text{O})^+$ .

Among the second class of molecular compounds, those with strong intramolecular forces, frozen  $\text{Ni}(\text{CO})_4$  represents the extreme situation in which intermolecular forces are very weak. The positive SIMS spectrum of  $\text{Ni}(\text{CO})_4$  contains  $(\text{Ni}(\text{CO})_4)^+$ , smaller ions like  $\text{CO}^+$ ,  $\text{Ni}^+$ ,  $(\text{NiCO})^+$ ,  $(\text{Ni}(\text{CO})_2)^+$ , and  $(\text{Ni}(\text{CO})_3)^+$  and larger ions like  $(\text{Ni}(\text{CO})_5)^+$  and  $(\text{Ni}(\text{CO})_6)^+$ . Other ions include  $\text{C}^+$ ,  $\text{O}^+$ ,  $\text{O}_2^+$ ,  $(\text{CO}_2)^+$ ,  $(\text{NiO})^+$ ,  $(\text{Ni}_2\text{O})^+$ ,  $(\text{NiC}_2\text{O}_3)^+$ , and  $(\text{NiC}_3\text{O}_4)^+$ .<sup>56</sup> Rabalais suggests that the molecular ion  $(\text{Ni}(\text{CO})_4)^+$  and some smaller ions can be ejected intact and then fragment to yield lower mass species, react in the selvedge to form larger ions and rearrangement products. The SIMS spectrum of frozen benzene<sup>136,137</sup> shows similar fragmentation and clustering. Ions of this sort appear in lower yields than ions formed from more polar molecules, and this is attributed to a greater probability for neutralization as a result of fairly broad band structures in the nonpolar solids.<sup>22</sup>

The probability of ionization is determined in Rabalais's view by the ease with which electron transfer can take place, and the band structure indicates how likely these transfers will be. Though there are criticisms of band structure models (see section III), these sorts of models are qualitatively useful and broadly applicable. The strengths of inter- and intramolecular forces can affect the mass spectra, with large clusters composed of individual molecules being favored for molecules with large intermolecular forces. Ion-molecule reactions in the selvedge account for many of the cluster and rearrangement ions observed. The concept of interaction strengths can also be extended to molecule-substrate interactions; intact emission will be favored for chemisorbed species, in agreement with Benninghoven, while recombination will be favored for physisorbed species, in agreement with Winograd and Garrison.

An extensive SIMS study of atoms and small molecules in frozen matrices has been undertaken by Michl and co-workers,<sup>136,147-154</sup> and Michl has proposed a detailed mechanism for ion formation from these materials,<sup>154-157</sup> which he terms the *gas flow model*.<sup>156,157</sup> In agreement with the results of Rabalais,<sup>137</sup> the SIMS spectra of low-temperature solids are observed to contain numerous cluster ions. For example, the positive ion SIMS spectrum of solid NO obtained by 4-keV  $\text{Ar}^+$  bombardment<sup>149</sup> includes the clusters  $[\text{NO}(\text{N}_2\text{O}_3)_n]^+$ ,  $[\text{N}_2\text{O}(\text{N}_2\text{O}_3)_n]^+$ , and  $[\text{NO}_2(\text{N}_2\text{O}_3)_n]^+$ , where  $n = 0, 1, 2, \dots$ . Extensive aggregation of this sort is explained by Michl as arising via a thermal spike mechanism. In brief, the overall mechanism involves two time regimes: at very short times after primary ion impact ( $<10^{-12}$  s) collision cascades result in secondary ion formation, but at somewhat longer times ( $>10^{-12}$  s) thermal processes take on a dominant role. Ions arising from collision cascades are called "first batch" ions, while those emitted from thermal spikes are called "second batch" ions.

Michl's experimental observations may be summarized briefly: (1) Heavy, high-energy primary ions produce greater secondary ion yields and more fragmentation than do light, low-energy primary ions.<sup>149</sup> (2) Bombardment of frozen rare gases with light rare-gas primary ions produces doubly charged rare-gas ions.<sup>148</sup> (3) The kinetic energy distributions of parent and fragment ions are rather broad (5-20-eV half-width),

while the distributions of cluster ions are narrower (1–10-eV half-width) and have peaks shifted to lower energies.<sup>148–152</sup> (4) Clusters from molecular solids are usually formed with a central ion solvated by several molecules (see the nitrogen oxides above), and both the central ion and solvating molecule may have compositions quite different from that of the bulk solid.<sup>147,149,150,152</sup> (5) Spectra of solid mixtures with the same overall elemental composition as solids composed of a single compound (e.g., N<sub>2</sub> and O<sub>2</sub> vs. NO) are much different.<sup>149</sup> Likewise, spectra of molecules diluted with rare gases are different from those of neat molecules.<sup>136,150,151</sup>

There are a number of differences between Michl's proposals and the results expected of classical dynamics calculations. It should be realized that Michl deals with bulk, insulating solids, while most calculations are applied to the case of monolayer coverage on metals. Calculations are normally terminated near the end of the collision cascade, and thus any processes that may arise after this time are neglected. For insulators, charges in the bulk may not dissipate as they would for metals, and localized charges may thus be important in sputtering of bulk molecular solids. In general, there is agreement on the early stages of desorption. Collision cascades result in emission of secondary particles from the surface by momentum transfer. These particles—the first batch particles—may include some intact species as well as fragments formed at the surface. Michl argues that ions observed in this stage of desorption are formed by electronic excitation. In molecular solids, intramolecular interactions are quite strong, while intermolecular interactions are weaker. If this situation is assumed to be similar to that in the gas phase, where molecular ionization cross sections are large for keV collisions, electronic excitation is a likely process for these systems.<sup>155</sup> Electronic excitation in the sputtering of ices has recently been discussed by Brown and Johnson.<sup>158</sup>

It is clear that a mechanistic description based solely on collision cascade phenomena is inadequate,<sup>155,156</sup> and the low kinetic energies of cluster ions are best explained by the development of a thermal spike after the initial excitation. The fact that a mixture of N<sub>2</sub> and O<sub>2</sub> gives a different spectrum than NO suggests that, even in bulk materials, molecular identity is preserved in the sputtering process. A thermal regime is presumably created during quenching of the collision cascade as energy is transferred to the cold surroundings in the solid. The thermal spike contains hot atoms, molecules, and ions, *but the spike is too short-lived to be at chemical equilibrium*. An important aspect of this mechanism is the occurrence of kinetically controlled reactions similar to those in high-energy radiation chemistry. Charges are scavenged according to the ionization potentials and electron affinities of the species in the spike. As the spike spreads, second batch particles are ejected in an "explosive expansion of high-pressure gas into vacuum".<sup>155</sup> During this expansion, clusters can be formed by recombination, and molecular fragmentation can occur. Ionization is thought to originate in the spike, and neutralization is impeded by slow electron transfer at the insulator surface and by shielding of the central charge by solvation; in addition, band structure may break down in

the disordered sputtering region. The final phase of the mechanism is metastable decay of sputtered clusters,<sup>159</sup> including loss of solvent molecules from charged clusters.

Michl's ideas are similar to those of Rabalais, although Rabalais does not develop the thermal spike concept in detail. To summarize, molecular emission from bulk solids results primarily from thermal processes, and fragmentation results from both thermal (late) and collision cascade (early) processes. Gas flow from the hot spike into vacuum is an essential part of this mechanism. For the common situations of sputtering from liquid matrices or from multilayers of organics burnished on various substrates this mechanism may be the dominant process. Many matrix effects in molecular SIMS<sup>160,161</sup> can be explained with these concepts, as will be discussed below.

Cooks and co-workers<sup>13,162–167</sup> have presented views of the molecular SIMS mechanism that are in broad agreement with the Rabalais–Michl models. These conclusions are based in large part on chemical effects, such as the influence of chemical derivatization and of the sample matrix on the spectra, and on parallels with the collision-induced dissociation behavior of gas-phase molecular ions. The concepts of cationization in the selvedge, precharged ion emission, and metastable ion fragmentation are central to this work. The similar spectra obtained by SIMS, FAB, LD, and PD suggest that, independently of the initial form of energy deposition, at some point energy is present in a common form. This so-called "energy isomerization" has been proposed to involve energy transfer to low-energy vibrational and translational modes.<sup>162–164</sup> In common with Michl and Rabalais, the concepts of quasi-thermal emission and selvedge reactions are thought to be important. An additional feature—and one in opposition to the views of Winograd and Garrison—is that for organic samples examined under static conditions most fragmentation results from unimolecular decay of metastable ions in the free vacuum.

Results from a number of systems suggest that extensive mixing occurs during sputtering and that formation of adduct ions arises by recombination as opposed to intact ejection. The numerous experimental results obtained from compounds mixed with ammonium chloride<sup>160–164,168</sup> and carbon<sup>169</sup> also support a model in which extensive mixing (as well as ion/molecule reactions) takes place in the selvedge. Mixtures of NH<sub>4</sub>Cl with biological molecules like sucrose were found to give large amounts of intact, cationized molecules, while in the absence of NH<sub>4</sub>Cl useful spectra were not obtainable.<sup>161</sup> This applies to intimate mixtures deposited onto substrates from solution and also to physical mixtures of solids. In the same manner, increasing the ratio of NH<sub>4</sub>Cl to 1-cyclohexyl-2,4,6-triphenylpyridinium perchlorate causes a decrease in the abundance of the fragment resulting from cyclohexene loss relative to the abundance of the intact quaternary ammonium cation.<sup>160</sup> The advantages of using glutathione as a matrix in plasma desorption<sup>170</sup> may have similar origins; certainly the improvements in analytical performance show a considerable degree of parallelism. The SIMS work with matrix effects yielded estimates<sup>171</sup> of the total amount of analyte converted to gas-phase ions for precharged organics.

These are surprisingly high (as high as 0.1%) in the presence of matrix and orders of magnitude lower in its absence.

The effects of salt matrices on reducing fragmentation are interpreted<sup>160,172</sup> in terms of Michl's desorption/desolvation mechanism.<sup>155,156</sup> For a quaternary ammonium salt,  $C^+A^-$ , mixed with  $NH_4Cl$ , emission from a thermal spike of a hot cluster of  $C^+$  solvated by several  $NH_4Cl$  species can be envisioned. The excited cluster sheds solvent molecules as it travels from the surface, and in the process excess energy is removed. The completely desolvated cation has less internal energy than it would have had if it had not been solvated. An alternative explanation of internal energy reduction by matrices is that collisional deexcitation of excited molecules takes place in the seldedge. Support for this idea comes from a FAB study which found that a single keV Xe atom could sputter as many as 1000 glycerol molecules.<sup>173</sup> Even if molecular yields in solid SIMS are much lower than this value, the possibility exists for many matrix-molecule collisions.

Further support for intimate mixing in the sputtering region comes from the observation that a physical mixture of the quaternary ammonium salt carnitine hydrochloride with  $NH_4Cl$  dramatically reduces the degree of intermolecular methyl transfer.<sup>162</sup> The positive SIMS spectrum of neat carnitine hydrochloride shows a molecular ion  $(M + H)^+$  and a more abundant ion  $(M + CH_3)^+$ . The latter ion is apparently formed by transfer of a methyl group from one carnitine molecule to another. Dilution with  $NH_4Cl$  gives a spectrum in which the product  $(M + CH_3)^+$  ion is suppressed. Emission of numerous  $NH_4Cl$  molecules or fragments would effectively prevent the intermolecular interactions of analyte necessary to promote methyl transfer. Note that in this and other cases where matrix effects suppress intermolecular reactions, the range over which mixing occurs appears to be large compared to the expected scale (*ca.* 100 Å) of a single sputtering event.

The question of fragmentation is addressed by Cooks with evidence garnered from tandem mass spectrometry (MS/MS).<sup>174</sup> In a typical experiment, a particular ion is mass-selected and then collisionally activated. Ionic dissociation products (daughter ions) are subsequently mass-analyzed. The daughter spectrum is thus the mass spectrum of a selected parent ion. Early experiments<sup>19,162</sup> demonstrated a correlation between fragmentation in SIMS and in the daughter spectra of ions generated in the gas phase. For example, the SIMS spectrum of phthalimide supported on copper contains a fragment ion  $(M + H - H_2O)^+$ , while the daughter spectrum of phthalimide protonated by chemical ionization contains the identical fragment ion.<sup>162</sup> Numerous other examples of similar fragmentation in both SIMS and collisional activation have been collected, as shown in studies of anthracene,<sup>19</sup> 1,4-dicyanobenzene,<sup>19</sup> *p*-aminobenzoic acid,<sup>19</sup> benzamide,<sup>162</sup> *p*-acetanisidide,<sup>162</sup> sucrose,<sup>166</sup>  $Co(acac)_3$  (*acac* = acetylacetonate),<sup>175</sup> and silver propionate.<sup>176</sup> The similarities have been interpreted as evidence that fragmentation in molecular SIMS is largely due to dissociation in the gas phase and not at the surface.

In the above cases, the fragment ions in SIMS and in the daughter spectra do not usually match perfectly, presumably due to the fact that the comparisons are

indirect; that is, generation of ions was not by SIMS in the MS/MS studies. There have since been some particle bombardment MS/MS experiments.<sup>153,177-181</sup> In one system, *O*-methylcandicine chloride, both the SIMS spectrum and the daughter spectrum of the intact cation contain fragment ions formed by loss of trimethylamine.<sup>177</sup> In the daughter spectra of sugar-glycerol clusters formed by FAB, most of the ions are identical with those in the single-stage FAB spectrum.<sup>181</sup> Taken together, the MS/MS results strongly suggest that some intact, desorbed molecular ions in SIMS contain sufficient internal energy to fragment before reaching the detector. Gas-phase dissociations of alkali halide clusters are known to occur.<sup>182-184</sup> Dissociations of large biomolecules have also been detected.<sup>185,186</sup> These conclusions are based on the observation of metastable ions in both time-of-flight and sector instruments. Recent <sup>252</sup>Cf-PDMS time-of-flight experiments in which neutrals and ions are detected simultaneously<sup>187</sup> have demonstrated unequivocally that molecules like the nucleoside guanosine can dissociate in the gas phase. There is really no longer a question as to whether gas-phase dissociations occur in molecular SIMS, but there is a question of how much surface vs. gas-phase fragmentation goes on and what systems favor one type of dissociation process over the other.

Insights into the SIMS mechanism also come from the studies of many other investigators whose work is not easily categorized in the framework of this review. Typical of this are Gardella's studies of cationization in monolayer samples prepared by the Langmuir-Blodgett technique,<sup>189</sup> Ross and Colton's work on matrix-assisted SIMS,<sup>169</sup> and Busch's use of MS/MS to study whether cluster ions are generated from organometallic compounds by intact ejection or by recombination.<sup>188</sup> Mechanistic insights are also to be found in the unexpected transformations which occur at the interface. These processes, for example, Michl's observations on nitrogen oxides, have done much to shape our thinking regarding SIMS mechanisms. The occurrence of transmethylation reactions of organic analytes has already been mentioned. As a bimolecular process, it provides a guide to the probability of ionic collisions between analyte molecules. A more unexpected but analogous reaction is the intermolecular N atom transfer which occurs for certain triazines.<sup>190</sup> This unusual process has been rationalized as a bimolecular seldedge reaction in which concerted electron redistribution yields the tetrazole product.

Unexpected reductions have also been reported,<sup>167,176</sup> and they yield further insights into processes occurring in the seldedge. The SIMS spectrum of thiophene adsorbed on silver is a case in point.<sup>191</sup> This spectrum contains the surprising ion  $(Ag + M + 4H)^+$ , which indicates that the thiophene molecule undergoes complete reduction to tetrahydrothiophene during the analysis. The series of ions  $(Ag + M + 4H - 14)^+$ ,  $(Ag + M + 4H - 28)^+$ , and  $(Ag + M + 4H - 42)^+$  is also unusual, since it must arise by extensive C-C bond cleavage of the tetrahydrothiophene skeleton. Other abundant ions include  $(AgH_xS)^+$  ( $x = 1-4$ ) and  $(Ag_2HS)^+$ . A likely source of hydrogen for the hydrogenation reaction is thiophene itself. A possible explanation of this behavior is that it is triggered by exceptionally strong bonding between sulfur and silver,

electrons for reduction being provided through the agency of the collision cascade itself. In a number of organometallic complexes the observation of fragments which arise by cleavage of strong C-C and C-N bonds provides evidence that the fragmenting molecule is not the monomer but a higher mass cluster species which may be ejected intact from the original surface into the selvedge.<sup>192</sup>

The preceding section has accentuated the differences between the collision cascade and vibrational or thermal models of ion emission. As ideas on the mechanism of SIMS have been refined a merging of models can be detected and it seems possible that common ground will be reached. For example, emission in the later stages of the collision cascade might be hard to distinguish from emission from a developing thermal spike.

## V. Mechanistic Insights from Other Desorption Ionization Techniques

### A. Mechanisms in FABMS and Liquid SIMS

Because FAB, PDMS, and LD give spectra similar to molecular SIMS, it is worthwhile to explore some of the mechanistic ideas advanced in these areas. If common ground can be found, it might enhance understanding of each of the different techniques. This section will consider FAB as an extension of SIMS, and much of the preceding molecular SIMS discussion applies also to FAB. On the other hand, there is an independent theoretical background for MeV particle bombardment effects. Finally, LD will be examined briefly and compared with particle bombardment methods.

As discussed above, FAB differs from SIMS only in the use of a neutral primary beam and a liquid matrix. Spectra obtained with ion beams and liquid matrices (liquid SIMS) are identical with FAB spectra,<sup>193</sup> and thus this discussion applies equally to liquid SIMS. A neutral primary beam is sometimes advantageous in studies of solid insulators because charge-induced damage can be minimized.<sup>194</sup> A similar effect with liquid matrices has not been reported, although liquid SIMS can give higher signals than FAB, presumably due to better focusing of charged-ion beams.<sup>193</sup> In the present context, the effect of the liquid matrix on desorption is the main factor to be considered. It is reasonable to suppose, as Magee has,<sup>83</sup> that a liquid and a solid surface will be virtually identical on the desorption time scale, even allowing for slow thermal effects. The concepts of collision cascades and thermal spikes remain valid, and it is quite probable that sputtering proceeds in a fashion analogous to that in the solid phase. The key points therefore reduce to (1) dissipation of primary particle energy by the matrix, (2) chemical effects of the matrix, and (3) what occurs in the (long) intervals between arrival of primary particles.

Kelner and Markey<sup>139</sup> and Kistemaker and co-workers<sup>195</sup> have obtained kinetic energy distributions of secondary organic ions in FAB and liquid SIMS. The former group found that kinetic energy maxima fall in the range 0-5 eV, with a very small high-energy tail. The latter obtained distributions, having full widths at half-maximum (fwhm), for glycerol clusters of the type  $[\text{glycerol}_n + \text{H}]^+$  that decrease from  $n = 1$  to 2 and then

increase for larger clusters. Distributions for  $\text{H}^+$  are extremely wide. Cluster ions of the type  $[(\text{NaCl})_n + \text{Na}]^+$  from samples of NaCl in glycerol show a steady increase in fwhm with increasing cluster size. Sputtering of solid NaCl produces clusters with much broader distributions than clusters sputtered from glycerol (2.2-eV fwhm vs. 0.7 eV,  $n = 3$ ). The intact cation of tetrabutylammonium iodide sputtered from glycerol has a fwhm equal to the fwhm values of its fragment ions. For a solid sample, distributions are broader and show more variation. Large organics like sucrose and the tripeptide Gly-Leu-Try sputtered from glycerol show small decreases in fwhm for fragment ions, and sucrose has smaller values of fwhm than does the tripeptide.

Kistemaker bases several conclusions on the above observations. The drastic lowering of fwhm values for  $\text{Na}^+$ , when sputtered from glycerol vs. from the solid, demonstrates that more low-energy particles can escape from glycerol, probably due to a lower ion-glycerol binding energy. The increase in fwhm as clusters grow larger is not understood, but the similarity between molecular and fragment ions is thought to indicate a low degree of unimolecular dissociation in the gas phase. This is a surprising result in view of the conclusions of other workers, whose data have already been discussed. The distributions are different from those of Garrison,<sup>130</sup> who noted a preference for fragment ions to have broader, higher energy distributions than molecular ions. It is interesting that two conflicting results are both interpreted as evidence for fragmentation at the surface. It should be noted in this context that kinetic energy distribution measurements have failed to resolve the question of whether alkali halide clusters are emitted directly or by recombination above the surface.<sup>9,196</sup>

Differences in *internal* energy of ions sputtered from liquid and solid matrices have been qualitatively evaluated by Cook and Chan.<sup>197</sup> These experiments compared the behavior of doubly charged organic ions (from diquatery ammonium salts) in spectra obtained with different desorption ionization techniques. Since the intercharge distance determines the intrinsic stability of such ions, fragmentation of different molecules can be used to study the amount of internal energy deposited by a given technique. Fragmentation was found to be much more extensive in FAB than in EHD ionization. Comparison with published SIMS spectra of the solids<sup>28</sup> revealed that fragmentation in FAB was smaller than in SIMS. A rough ordering of energy deposition is thus SIMS > FAB > EHD. Fragmentation in FAB is presumably minimized by the presence of excess solvent molecules. On the basis of observation of high-energy fragmentations in FAB,<sup>25</sup> however, it is apparent that deposition of considerable internal energy can occur in spite of the liquid matrix.

A common rationalization for the ability to sputter liquid matrices for a relatively long time while retaining the molecular information is that the liquid surface continually renews itself by diffusion.<sup>30</sup> Recent experiments<sup>173,198,199</sup> show that this may not be the case in high-flux experiments. FAB spectra of a mixture of glycerol- $d_5$  and glycerol- $d_8$ , where glycerol- $d_5$  is initially present at the surface, demonstrate that diffusion occurs very slowly; glycerol- $d_8$  does not give a larger signal than glycerol- $d_5$  until after about 1 min of bombard-

ment.<sup>198</sup> It is suggested that glycerol is removed in layers and that signal longevity arises in part by an entrainment mechanism in which the volatile glycerol carries large involatile molecules with it as it is rapidly vaporized by particle impact.<sup>198</sup> Thus, the solvent vapor pressure plays an important part in the FAB mechanism. This cluster emission model is quite similar to Michl's model<sup>155-158</sup> and to models for the thermospray technique used in LCMS.<sup>47</sup>

These ideas have been corroborated by experiments in which chemical noise associated with glycerol is monitored in relation to the signal-to-noise ratio of a molecular ion.<sup>173,199</sup> Both quantities decrease in parallel with bombardment time, although if diffusion were important one might expect to see an increase in chemical noise as radiation-damage products rediffuse back to the surface at longer sputtering times. This result suggests that the sputtering process in FAB involves removal of large amounts of material with each impact, including the products of radiation damage. Renewal of the surface by diffusion is therefore not required. Diffusion may be a factor in some instances, however, as indicated by a calculation<sup>200</sup> which shows that alkali metal cations may diffuse fast enough in glycerol to make FAB spectra diffusion-controlled.

The ion formation process in FAB and liquid SIMS is of great interest. While direct desorption of precharged species (e.g., ammonium salts, Na<sup>+</sup>, Cl<sup>-</sup>) is generally accepted, there is a debate much like that in SIMS of solids as to the origin of cationized or anionized molecules. Since specific solvents have been found effective for obtaining FAB spectra of different compound types,<sup>201,202</sup> there can be no doubt that matrix effects in the ionization process are substantial. A fundamental question is whether preformed ions are created prior to desorption by, for example, transfer of labile glycerol protons to dissolved molecules.<sup>203</sup> The prevalence of (M + H)<sup>+</sup> and (M - H)<sup>-</sup> ions can be taken as an indication that proton transfer occurs in the liquid matrix before sputtering. This is supported by the fact that addition of acids to liquid matrices can enhance yields of (M + H)<sup>+</sup>,<sup>204</sup> which is simply the solution-phase analogue to SIMS experiments in which protonated molecule emission is enhanced with acids.<sup>23</sup> In addition, the relative proton affinities of various solvents and carbohydrate molecules have been correlated with the occurrence of protonated species<sup>205</sup> and the formation of charge-transfer<sup>206</sup> and SbCl<sub>3</sub> complexes<sup>207</sup> in solution has been correlated with enhanced emission of analyte molecular ions. Other work has shown that alkali cation attachment in solution—either to the solvent or to the analyte—may be an important process in the FAB mechanism,<sup>181,200</sup> even though seldge cationization may also be operative.

In contrast to the simple transfer reactions that produce preformed even-electron ions in solution, the production of radical intermediates can explain some of the behavior observed in FAB.<sup>208</sup> Bombardment of systems without labile protons may produce radical cations, which may subsequently abstract hydrogen atoms from other molecules. Proton transfer from these ions to neutral molecules might then be possible. This very behavior was observed in a FAB study of glycerol-*d*<sub>5</sub>.<sup>208</sup> Here the glycerol is deuteriated on the carbon atoms, and not on the oxygen atoms; hence, there are

no labile deuterons. The FAB spectrum of glycerol-*d*<sub>5</sub>, however, contains an (M + D)<sup>+</sup> peak more intense than the sum of the natural isotopic contribution of (M + H)<sup>+</sup> at this mass, even though direct transfer of deuterons is clearly impossible. A plausible explanation is that glycerol radical cations are created by primary radiation damage, and these radicals abstract deuterium from carbon to form (glycerol + D)<sup>+</sup> ions. Additional evidence for this mechanism comes from the report of extensive radical formation in glycerol by particle bombardment.<sup>209</sup>

A radical formation mechanism is probably not responsible for most of the ions observed in FAB, but it is apparently important in many cases. As noted earlier, polycyclic aromatic hydrocarbons give abundant radical cations in FAB.<sup>25</sup> The reduction of quinone antibiotics in FAB<sup>210</sup> probably represents another occurrence of electron transfer. Numerous bombardment-induced reactions within liquid matrices have been reported,<sup>211</sup> and many of these also must involve high-energy primary damage processes.

Kebarle<sup>212</sup> has investigated the role of gas-phase basicities in FAB, and from this work he has drawn conclusions about the relative contributions of preformed ion ejection vs. ionization by ion/molecule reactions in the gas phase. In a mixture of compounds that have a low degree of ionization in the liquid phase, molecules with higher gas-phase basicities generally gave more (M + H)<sup>+</sup> ions than did molecules with lower gas-phase basicities. The occurrence of collisions in the seldge explains the preference for protonation based on gas-phase basicities. Because the samples were specifically designed not to favor precharged-ion formation, it seems inappropriate to conclude<sup>212</sup> that ejection of precharged ions is not a significant SIMS/FAB mechanism.

To summarize the FAB mechanism, it should first be noted that the physics behind desorption is virtually identical with that in SIMS of solids and liquids. Liquid matrix effects are therefore the key mechanistic factors. The common ionization types—direct desorption of precharged materials, cationization/anionization, and radical formation—occur in FAB as in SIMS, although radical chemistry is much more important in the liquid phase and the presence of a solvent often has its own unique influence on the type of ion eventually emitted. It seems likely that desorption of large numbers of particles, including solvated clusters, takes place.<sup>173,181,199</sup> Nondestructive emission of molecules is the result of mitigation of the primary impact energy by the solvent, while signal longevity is due to the continuous presence of fresh material at the interface. There is not yet complete agreement on whether the collision cascade (directed translational motion) or the thermal spike (random translational and vibrational) models best describe FAB; the evidence seems to favor the latter.

## B. Mechanisms in Other Desorption Ionization Techniques

While both SIMS and PDMS are particle bombardment methods, PDMS employs primary ions with kinetic energies 3-5 orders of magnitude higher than those used in SIMS. This causes fundamental differences in the way energy is initially deposited.<sup>32,213-216</sup> As



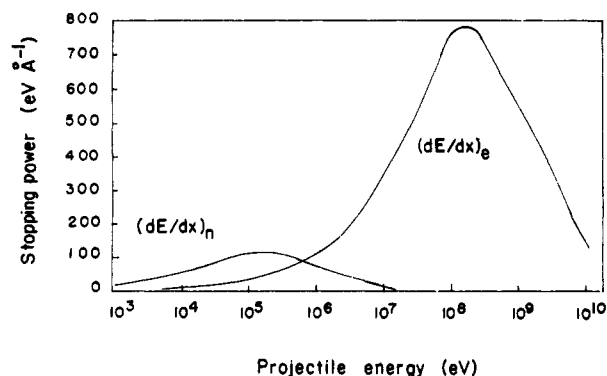


**Figure 6.** Energy deposition ( $dE/dx$ ) as a function of collision energy showing relative contributions from nuclear (n) and electronic (e) excitation (from ref 32).

illustrated in Figure 6 for the case of sputtering of an organic compound by  $^{99}\text{Tc}$ , nuclear stopping (vibrational excitation) is important in the primary ion energy range of  $10^3$ – $10^7$  eV, while electronic stopping is important in the range  $10^5$ – $10^{10}$  eV.<sup>32</sup> A similar plot has also been published for sputtering of Nb by  $^{79}\text{Br}$ .<sup>215</sup> In simple terms, keV-energy ions lose most of their energy through collisions with atomic nuclei in the target, while MeV-energy ions—which move faster than electrons in the hydrogen atom—lose energy through collisions with electrons in the target. It is therefore necessary to explain how this electronic excitation is converted into a form such that molecular ions can be desorbed, as well as how the emission processes induced by keV and MeV primary ions overlap.

A comparison of the positive and negative secondary ion and  $^{252}\text{Cf}$ -PD mass spectra of eight different compounds having molecular weights below 2000 dalton demonstrated a remarkable similarity between the two techniques,<sup>217</sup> even though the spectra were obtained with different time-of-flight mass spectrometers. A more controlled comparison of desorption yields for 54-MeV  $^{63}\text{Cu}^{9+}$  and 3-keV  $^{133}\text{Cs}^+$  measured by using the same instrument has established differences between high- and low-energy sputtering.<sup>218</sup> Five molecules, ranging in mass from 133 to 1884 dalton, were studied. The results consistently indicate that yields in high-energy experiments are greater than in low-energy experiments and that this effect becomes *more* pronounced at higher masses. For example, the ratio of the high-energy yield to the low-energy yield for glycylglycine (mol wt = 132) is  $13.7 \pm 0.5$ , while the ratio for bleomycin (mol wt = 1375) is  $223 \pm 25$ . Recent experiments<sup>219</sup> show that approximately 100 leucine molecules can be desorbed by a single 90-MeV  $^{127}\text{I}^{14+}$  impact. These results imply that an MeV particle can excite a larger area, or put more energy into a given area, than can a keV particle, increasing the chances of desorbing a large, extended molecule.

Several other differences between sputtering with keV and MeV particles have been reported. For MeV ions, the charge state has a critical effect on the ion yield.<sup>220</sup> The yields of  $(M + H)^+$  from glycylglycine and  $M^{+}$  from ergosterol increase approximately eightfold as the charge on 20-MeV oxygen is increased from +2 to +8.<sup>220</sup> The data suggest that the yield varies as a function of the electronic stopping power  $(dE/dx)_e$ —specifically as  $(dE/dx)_e^2$ . Another difference is the observation of positively charged ions of electronegative

atoms like  $\text{O}^+$ ,  $\text{F}^+$ ,  $\text{S}^+$ , and  $\text{Cl}^+$  in 70-MeV  $^{79}\text{Br}^{7+}$  bombardment of a solid.<sup>215</sup> The well-known dependence in keV sputtering of positive ion yields on ionization potentials<sup>69–71</sup> seems not to hold for MeV sputtering. Finally, background noise is eliminated more effectively in MeV bombardment than in keV bombardment by use of an energy prefilter, suggesting that high-energy bombardment produces secondary ions with lower kinetic energies<sup>215</sup> (but not necessarily lower *internal* energies).

These differences—especially the preference for electronic stopping over nuclear stopping in MeV bombardment—indicate that collision cascades are relatively unimportant in PDMS. One might then be tempted to dismiss PDMS as irrelevant to the discussion of SIMS, but the similar ion types in the spectra demand consideration. Moreover, thermal models for PDMS have been proposed,<sup>221–226</sup> and these may bear directly on the thermal models proposed in SIMS. An early model for  $^{252}\text{Cf}$ -PDMS of CsBr<sup>221</sup> postulated that the fission fragment track, produced by electronic motion and consisting of a hot core (ca. 25 Å in radius,  $6.6 \times 10^4$  K) surrounded by an outer sheath (ca. 100 Å in radius), causes ion emission by rapid evaporation at the point where it meets the surface. Note that this sounds very similar to the thermal spike model of SIMS. Such a model could apply to molecules as well, since rapid heating will tend to favor evaporation over fragmentation (recall desorption chemical ionization).<sup>46,227</sup> Similar ideas have been advanced in terms of a *Coulomb explosion model*,<sup>222,224</sup> in which ions are emitted from the damage track as a result of Coulombic repulsions. This model is compatible with the observed  $(dE/dx)_e^2$  relationship<sup>220</sup> mentioned earlier. Because neutralization prior to emission was thought to be probable in this model, however, another group proposed a thermal spike model of emission.<sup>225</sup> A precise description of the conversion of electronic motion into heat has not been achieved. One possibility is that Coulombic repulsions within the damage track equilibrate to a thermal spike<sup>223</sup> in a process somewhat reminiscent of spike formation by collision cascades.

A different approach to the PDMS mechanism centers around electronic, rather than thermal, effects. Sundqvist and co-workers<sup>214,228–230</sup> are the proponents of an electronic model (the *ion-track model*) involving multiple simultaneous bond-breakage events. Bonds are postulated to be ruptured by secondary electrons produced in the damage track, and molecular emission occurs if a number of intermolecular bonds are broken at the same time. As the electronic stopping power is increased by increasing the primary ion energy, its charge, and its mass, secondary ion yields are expected to increase in turn, since the number of secondary electrons produced will increase. This in fact is observed experimentally.<sup>229</sup> The critical parameter affecting desorption is thus the density of the deposited energy. If the density is high and is spread over an area much smaller than the dimensions of a particular molecule, fragmentation will be likely.

The experimental results for PDMS indicate quite clearly that the technique differs in many ways from SIMS. If the thermal rather than the ion-track description of PDMS is valid, however, then the spectral similarities between keV and MeV sputtering are ex-

plained quite simply, since thermal processes appear to contribute to desorption in keV sputtering in molecules. The ion-track model, on the other hand, resembles in some ways the "concerted push" mechanism of Garrison and Winograd; both require simultaneous bond-breaking processes, even though the latter occurs as a result of collision cascades. The ionization process has not been dealt with explicitly here, but it is probably reasonable to assume that seldge recombination, precursor formation, solvated-cluster emission, and the other SIMS ionization models all apply; recent experiments with nitrocellulose substrates suggest that precursor formation can indeed contribute to ionization in PDMS.<sup>231</sup> Even multiply charged precursors are emitted in high yields. A thermal desorption model fits the notion of isomerization of energy to the same form as for other DI experiments. In the next paragraphs, it will be seen that a thermal model for LD appears to be the most satisfactory. The pervasiveness of thermal (vibrational) models for desorption ionization suggests that such a model is important in molecular SIMS.

Laser desorption is distinguished from SIMS, FAB, and PDMS in that it is not based on particle bombardment. As in PDMS, momentum transfer is negligible. LD mass spectra often closely resemble particle bombardment mass spectra.<sup>166,232-235</sup> As with other desorption ionization methods, the LD mechanism has been debated extensively. The majority of workers advocate a thermal mechanism, but a nonthermal model has also been suggested to operate in some circumstances.<sup>236-238</sup>

Conzemius and Capellen<sup>37</sup> have reviewed the LD literature through 1979 in depth, and Hillenkamp<sup>236</sup> has summarized the experimental parameters employed in several laboratories. Several characteristics of the method can be noted. The laser wavelength is generally not important, but the laser power density is extremely important. Below about  $10^8$  W cm<sup>-2</sup> the ratio of ions to neutrals is very low (ca.  $10^{-5}$ ). Above  $10^9$  W cm<sup>-2</sup>, however, ionization is quite efficient but is accompanied by extensive sample decomposition. Continuous wave (CW) lasers seem to be a special case because of their low power densities, and perhaps the ionization mechanism with these lasers is strictly thermal evaporation.<sup>236,238</sup>

One of the earliest observations of mechanistic significance in LD is the continued emission of neutral species for several microseconds after a laser pulse is terminated.<sup>239</sup> This delayed desorption phenomenon has since been shown to apply to ion emission as well.<sup>166,240-245</sup> Ejection of sucrose ions was observed to occur for about 300  $\mu$ s after a 10-ns laser pulse (power density  $10^8$  W cm<sup>-2</sup>).<sup>166</sup> Cotter<sup>241,242</sup> monitored ion signals from (CH<sub>3</sub>)<sub>4</sub>N<sup>+</sup>Cl<sup>-</sup> at intervals up to 500  $\mu$ s after a 40-ns laser pulse. The intensities of the ions Na<sup>+</sup>, K<sup>+</sup>, and ((CH<sub>3</sub>)<sub>4</sub>N)<sup>+</sup> peaked at times of 5-15  $\mu$ s after the pulse, and these ions were not detected after 50  $\mu$ s. The neutral species (CH<sub>3</sub>)<sub>3</sub>N and CH<sub>3</sub>Cl could be detected even after 500  $\mu$ s by use of electron ionization. Emission of very large ions can also continue for long times after the laser pulse; for example, the (M + H)<sup>+</sup> ion of trehalose octapalmitate (mol wt = 2246 amu) was observed 10  $\mu$ s after a 40-ns laser pulse.<sup>244</sup>

Results like those just described are suggestive of thermal emission processes. Calculations indicate a

slow falloff (microsecond regime) in the surface temperature after it is elevated by a laser pulse,<sup>246</sup> associated with the much larger volume of the hot spot as compared with particle desorption methods. This long-lived temperature elevation may be responsible for the longevity of ion and neutral emission. In fact, quaternary ammonium and phosphonium salts,<sup>247</sup> potassium salts of carboxylic acids,<sup>248</sup> and mixtures of alkali halides with a crown ether, glucose, and adenosine<sup>248</sup> are found to produce M<sup>+</sup> and (M + alkali)<sup>+</sup> ions when resistively heated. (M + alkali)<sup>+</sup> ions produced by resistive heating and by LD are generally thought to arise from gas-phase combination of evaporated neutral molecules with alkali ions.<sup>248-250</sup> High temperatures at the center of the laser spot may be responsible for alkali ion emission, while cooler areas further from the spot center may be the source of the organics. Experiments in which molecules are physically separated from alkali cation sources have demonstrated that gas-phase cationization is indeed possible,<sup>249,250</sup> although other ionization processes are not ruled out.

It has been found that *radical ions* such as M<sup>•+</sup> from anthracene can also be formed by a process with a thermal component.<sup>251</sup> Neutral anthracene is evaporated by heating, and free molecules are photoionized by the laser beam above the surface. The experimental evidence for this process includes a wavelength dependence on ion emission, and, 2  $\mu$ s after the laser probes the surface, a large increase in ion current when a second laser irradiates the area just above the surface. A similar effect has been reported in FAB<sup>252</sup> and SIMS.<sup>253</sup> Neutral organic molecules were shown to ionize by collisions with the primary beam.<sup>253</sup>

As is the case for SIMS and FAB, kinetic energy distributions of ions in LD have been used to gain mechanistic insights.<sup>243,254-256</sup> The kinetic energy distribution of K<sup>+</sup> from KCl was found to be about 15 eV wide 10  $\mu$ s after the laser pulse, but only about 0.3 eV wide 43  $\mu$ s after the laser pulse.<sup>243</sup> The low energy spread at long delays is consistent with an equilibrium thermal model, but energies of 10 eV or more suggest a nonequilibrium process. A study of Na<sup>+</sup> and (Na + sucrose)<sup>+</sup> distributions<sup>256</sup> showed peak widths greater than 1 eV for both ions, with the (Na + sucrose)<sup>+</sup> distribution being slightly broader than that of Na<sup>+</sup>. These distributions are much wider than that obtained for thermionic Na<sup>+</sup> emitted from a 1000 K substrate. The ion "temperature" required to produce the observed (Na + sucrose)<sup>+</sup> distribution was calculated to be between 3000 and 3300 K. This extremely high temperature suggests a nonequilibrium process, since survival of such a hot molecule under equilibrium conditions is unlikely.

Hillenkamp<sup>236,238</sup> divides the LD mechanism into four separate processes. The first two—thermal evaporation of ions and gas-phase combination of ions and neutrals—are generally accepted and have been the major focus of the discussion in this section. The third process is not useful for organic analysis. It occurs at high power densities ( $>10^{10}$  W cm<sup>-2</sup>) and involves formation of hot plasmas that destroy molecular identity. The fourth process is referred to as "true" laser desorption.<sup>236</sup> This could be called the analogue to such high-energy processes as collision cascades in SIMS

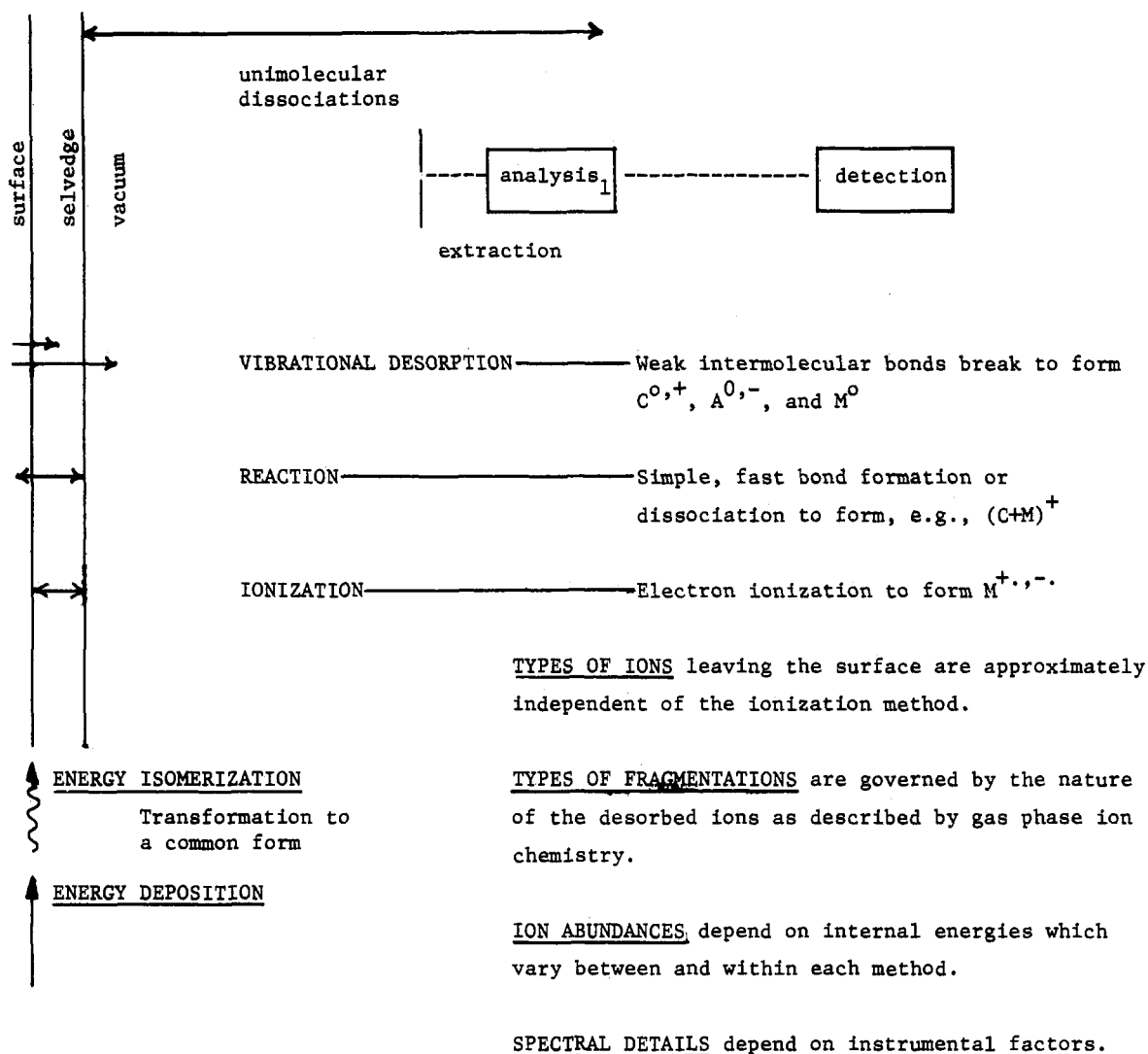


**Figure 7.** Early proposal of a unified model for SIMS and other desorption ionization experiments. Reproduced with permission from ref 164. Copyright 1983 Elsevier. (First presented at a conference on ion formation from organic solids, Münster, West Germany, 1981.)

because its existence is indicated by the high kinetic energies of some laser-desorbed ions. Furthermore, cluster-ion emission from materials like pure graphite does not occur by heating, yet it does occur in LD.<sup>257</sup>

Krueger<sup>237</sup> has formulated a model to handle instances of nonthermal emission in LD. The model is specific for alkali halides but may be applicable to polar organic molecules as well. It is important to realize that a photon beam contains energy yet lacks appreciable momentum, and hence the primary excitation process in LD must be different from that of either SIMS or PDMS. Krueger suggests that multiphoton absorption, leading to population of the conduction band, is the primary excitation step in LD of alkali halides (which are transparent). Energy transfer to the lattice by interactions of conduction band electrons and phonons (rapid, adiabatic heating) results in ion emission. The types of ions eventually emitted resemble those emitted by quite disparate primary excitation techniques, and thus the energy isomerization concept can again be invoked.

In a given LD experiment, both thermal and non-thermal processes may occur. As Hillenkamp remarks, "It is quite likely...that under a suitable choice of experimental parameters in laser desorption with high

power lasers one can simultaneously create a plasma in the center of the non-uniformly irradiated area, get 'true' laser desorption from the periphery, and even thermal emission due to a heated substrate for times longer than the laser pulse".<sup>236</sup> The later stages of ion emission in LD are probably very much like those in SIMS and FAB, since, for example, cationized molecules, clusters, and fragment ions are all observed. In addition, the use of ammonium chloride<sup>258</sup> or glycerol<sup>259</sup> matrices in LD stabilizes and enhances yields of organic ions, just as is the case for SIMS and FAB.

### C. Unified Description of Desorption Ionization

Mention is often made of the similarities among the spectra obtained with different desorption ionization techniques, yet few workers have attempted to unify the techniques with a common model. Certainly differences exist in the methods, particularly in the energy deposition process. We have used<sup>162,164</sup> the general term "energy isomerization" to describe the conversion of energy from its initial form into the form that results in emission of common ion types. Michi<sup>155,157</sup> later described this more explicitly. In order to unify all the methods, a thermal component is the obvious—and

perhaps the only—choice. SIMS, PDMS, and LD are so different initially that it is difficult to reconcile the spectral characteristics as arising by sheer coincidence from three different processes.

Some years ago many of these ideas were incorporated into an overall description of molecular SIMS (and related techniques). This description appears to retain some value and is presented again in Figure 7. These ideas center on a vibrational desorption mechanism as opposed to translational desorption arising directly from collision cascades.

Brief reference is now made to the work of three groups who start with thermal excitation and attempt to account for particle and laser desorption. One of these, Vestal, has proposed a unified, qualitative model based in large part on thermal spikes.<sup>260</sup> The interesting feature of Vestal's ideas is that they attempt to explain molecular ion formation in the thermospray technique as well as in particle bombardment and emphasize the similarities between these techniques.

Krueger<sup>261,262</sup> has derived expressions that account for the spectra resulting from fast energy-transfer processes such as particle and photon bombardment. This treatment ignores the details of excitation and considers the important parameters to be the vibrational frequencies of the modes to be excited, dielectric coupling strengths, and the total action of the perturbation. The action is a measure of the degree of excitation and affects the absolute yield of emitted species. Emission is described as the result of a nonequilibrium surface-gas-phase transition induced by a sudden perturbation of the sample electron plasma. Despite the neglect of the actual physical processes resulting in excitation, Krueger's calculations do predict a preference for non-radical species, emission of preformed ions, and cationization at the surface (precursor formation).

Tsong and Lin<sup>263,264</sup> have developed a method based on a "noncascade" sputtering model (vibrational excitation) for predicting ion yields and kinetic energy distributions using RRKM theory.<sup>265</sup> It can be applied to most desorption ionization techniques, including SIMS, FAB, PD, and LD. It is assumed that desorption occurs without charge transfer; i.e., ions are preformed. Upon excitation of a specific surface region, the distribution of sputtered products is determined by the amount of energy deposited into each vibrational mode and the activation energies for emission of products. In analogy to the usual gas-phase RRKM treatment, the more energy deposited, the greater the reaction rate; the lower the activation energy, the greater the yield of particles.

In conclusion, with respect to molecular SIMS, the most important mechanistic question appears to concern the relative contributions of ejection due to momentum transfer or to thermal effects. In atomic SIMS many factors (including kinetic energy distributions, angular effects, and agreement with linear cascade theory) point to a momentum-transfer mechanism. In molecular SIMS, momentum transfer appears to play a secondary role in ion emission. The type of sample is an important factor in determining the sort of mechanism that will operate in a given experiment. For thin films on metallic substrates, direct momentum transfer may be dominant. For multilayers, momentum transfer undoubtedly takes place, but it is followed by

thermal effects that ultimately have a greater influence on the spectra. Turning to the ionization process, as opposed to the particle ejection process, there is no dispute over the fact that chemical effects are dominant in molecular SIMS. Electron- and proton-transfer processes, where they lead to ion emission, often involve chemical reactions with matrix species rather than simple ionization. It seems likely that more cases of interesting interfacial chemical reactions will be uncovered as a wider range of analytes and matrices are utilized.

If a single, concise conclusion could be drawn concerning the mechanism of molecular SIMS, it would be the following: ion emission is initiated by momentum-transfer processes, and some atomic and molecular species are sputtered by momentum transfer. The momentum transfer eventually leads to a translationally and vibrationally excited mobile conglomeration of target components. This system moves toward thermal equilibrium while ion ejection occurs continuously. Within this dynamic region, known as the selvedge, extensive mixing occurs. Association (ion/molecule) and dissociation reactions occur and lead to new ionic species including molecular ions, cationized molecules, clusters, and fragment ions. Some preformed ions move through the selvedge without fragmentation or reaction. The nature of the sample, including chemical factors such as matrix components and physical factors such as the hardness of the surface, has a profound influence on the population of ions emitted. New species are often simple adducts or fragments of the original analyte, but in some cases more complex surface reactions can be promoted. Some clusters and ions may have sufficient internal energy to fragment in the gas phase. Fragment ions arise principally from such metastable precursors.

*Acknowledgments.* This work was supported by National Science Foundation Grant CHE 84-08258. Nick Delgass, Barbara Garrison, and Josef Michl provided valuable comments.

## References

- (1) Grove, W. R. *Philos. Mag.* **1853**, *5*, 203.
- (2) Thomson, J. J. *Philos. Mag.* **1910**, *20*, 752.
- (3) Honig, R. E. Retrospective Lectures, 32nd Annual Conference on Mass Spectrometry and Allied Topics, San Antonio, TX, 1984; p 19.
- (4) Wehner, G. K. *Phys. Rev.* **1956**, *102*, 690.
- (5) Honig, R. E. *J. Appl. Phys.* **1958**, *29*, 549.
- (6) Burlingame, A. L.; Baillie, T. A.; Derrick, P. J. *Anal. Chem.* **1986**, *58*, 165R.
- (7) Sigmund, P. *Phys. Rev.* **1969**, *187*, 768.
- (8) Holland, J. F.; Soltmann, B.; Sweeley, C. C. *Biomed. Mass Spectrom.* **1976**, *3*, 340.
- (9) Honda, F.; Lancaster, G. M.; Fukuda, Y.; Rabalais, J. W. *J. Chem. Phys.* **1978**, *69*, 4931.
- (10) Benninghoven, A. *Surf. Sci.* **1971**, *28*, 541.
- (11) Benninghoven, A.; Rüdener, F. G.; Werner, H. W. *Secondary Ion Mass Spectrometry*; Wiley: New York, 1987.
- (12) Busch, K. L. *Methods of Surface Analysis*; Czanderna, A. W., Hercules, D. M., Eds.; Plenum: New York, in press.
- (13) Day, R. J.; Unger, S. E.; Cooks, R. G. *Anal. Chem.* **1980**, *52*, 557A.
- (14) Colton, R. J.; Ross, M. M.; Kidwell, D. A. *Nucl. Instrum. Methods Phys. Res., Sect. B* **1986**, *13*, 259.
- (15) Day, R. J.; Unger, S. E.; Cooks, R. G. *J. Am. Chem. Soc.* **1979**, *101*, 501.
- (16) Unger, S. E.; Ryan, T. M.; Cooks, R. G. *Anal. Chim. Acta* **1980**, *118*, 169.
- (17) Benninghoven, A.; Jaspers, D.; Sichtermann, W. *Appl. Phys.* **1976**, *11*, 35.
- (18) Grade, H.; Winograd, N.; Cooks, R. G. *J. Am. Chem. Soc.* **1977**, *99*, 7725.

- (19) Grade, H.; Cooks, R. G. *J. Am. Chem. Soc.* 1978, 100, 5615.
- (20) Benninghoven, A.; Sichtermann, W. *Anal. Chem.* 1978, 50, 1180.
- (21) Day, R. J.; Unger, S. E.; Cooks, R. G. *J. Am. Chem. Soc.* 1979, 101, 499.
- (22) Murray, P. T.; Rabalais, J. W. *J. Am. Chem. Soc.* 1981, 103, 1007.
- (23) Busch, K. L.; Unger, S. E.; Vincze, A.; Cooks, R. G.; Keough, T. *J. Am. Chem. Soc.* 1982, 104, 1507.
- (24) Ross, M. M.; Colton, R. J. *Anal. Chem.* 1983, 55, 150.
- (25) Dube, G. *Org. Mass Spectrom.* 1984, 19, 242.
- (26) Hambitzer, G.; Heitbaum, J. *Anal. Chem.* 1986, 58, 1067.
- (27) Liu, L. K.; Unger, S. E.; Cooks, R. G. *Tetrahedron* 1981, 37, 1067.
- (28) Ryan, T. M.; Day, R. J.; Cooks, R. G. *Anal. Chem.* 1980, 52, 2054.
- (29) Barber, M.; Bordoli, R. S.; Sedgwick, R. D.; Tyler, A. N. *J. Chem. Soc., Chem. Commun.* 1981, 325.
- (30) Barber, M.; Bordoli, R. S.; Elliott, G. J.; Sedgwick, R. D.; Tyler, A. N. *Anal. Chem.* 1982, 54, 645A.
- (31) Torgerson, D. F.; Skowronski, R. P.; Macfarlane, R. D. *Biochem. Biophys. Res. Commun.* 1974, 60, 616.
- (32) Sundqvist, B.; Macfarlane, R. D. *Mass Spectrom. Rev.* 1985, 4, 421.
- (33) Håkansson, P.; Kamensky, I.; Sundqvist, B.; Fohlman, J.; Peterson, P.; McNeal, C. J.; Macfarlane, R. D. *J. Am. Chem. Soc.* 1982, 104, 2948.
- (34) Dück, P.; Treu, W.; Fröhlich, H.; Galster, W.; Voit, H. *Surf. Sci.* 1980, 95, 603.
- (35) Håkansson, P.; Kamensky, I.; Sundqvist, B. *Nucl. Instrum. Methods* 1982, 198, 43.
- (36) Della Negra, S.; Jacquet, D.; Lorthiois, I.; LeBeyec, Y.; Becker, O.; Wien, K. *Int. J. Mass Spectrom. Ion Phys.* 1983, 53, 215.
- (37) Conzemius, R. J.; Capellen, J. M. *Int. J. Mass Spectrom. Ion Phys.* 1980, 34, 197.
- (38) Honig, R. E.; Woolston, J. R. *Appl. Phys. Lett.* 1963, 2, 138.
- (39) Vastola, F. J.; Mumma, R. O.; Pirone, A. J. *Org. Mass Spectrom.* 1970, 3, 101.
- (40) Posthumus, M. A.; Kistemaker, P. G.; Meuzelaar, H. L. C.; Ten Noever de Brau, M. C. *Anal. Chem.* 1978, 50, 985.
- (41) Winograd, N.; Baxter, J. P.; Kimock, F. M. *Chem. Phys. Lett.* 1982, 88, 581.
- (42) Cotter, R. *Anal. Chem.* 1980, 52, 1767.
- (43) Honig, R. *J. Appl. Phys.* 1958, 29, 549.
- (44) Beckey, H. D. *Principles of Field Ionization and Field Desorption Mass Spectrometry*; Pergamon: New York, 1977.
- (45) Simons, D. S.; Colby, B. N.; Evans, C. A., Jr. *Int. J. Mass Spectrom. Ion Phys.* 1974, 15, 291.
- (46) Baldwin, M. A.; McLafferty, F. W. *Org. Mass Spectrom.* 1973, 7, 1353.
- (47) Vestal, M. L. *Mass Spectrom. Rev.* 1983, 2, 447.
- (48) Whitehouse, C. M.; Dreyer, R. N.; Yamashita, M.; Fenn, J. B. *Anal. Chem.* 1985, 57, 675.
- (49) Wehner, G. K. *Phys. Rev.* 1957, 108, 35.
- (50) Andersen, C. A. *Int. J. Mass Spectrom. Ion Phys.* 1969, 2, 61.
- (51) Storms, H. A.; Brown, K. F.; Stein, J. D. *Anal. Chem.* 1977, 49, 2023.
- (52) Anderson, H. H.; Bay, H. L. In *Sputtering by Particle Bombardment I*; Behrisch, R., Ed.; Topics in Applied Physics 47; Springer-Verlag: Berlin, 1981; p 145.
- (53) Harrison, D. E., Jr.; Levy, N. S.; Johnson, J. P., III; Effron, H. M. *J. Appl. Phys.* 1968, 39, 3742.
- (54) Harrison, D. E., Jr.; Kelly, P. W.; Garrison, B. J.; Winograd, N. *Surf. Sci.* 1978, 76, 311.
- (55) Roosendaal, H. E. In *Sputtering by Particle Bombardment I*; Behrisch, R., Ed.; Topics in Applied Physics 47; Springer-Verlag: Berlin, 1981; p 219.
- (56) Almén, O.; Bruce, G. *Nucl. Instrum. Methods* 1961, 11, 257.
- (57) Stuart, R. V.; Wehner, G. K. *J. Appl. Phys.* 1962, 33, 2345.
- (58) Anderson, H. H.; Bay, H. L. *Radiat. Eff.* 1972, 13, 67.
- (59) Elich, J. J.; Roosendaal, H. E.; Onderdenlinden, D. *Radiat. Eff.* 1972, 14, 93.
- (60) Cheney, K. B.; Pitkin, E. T. *J. Appl. Phys.* 1965, 36, 3542.
- (61) Silsbee, R. H. *J. Appl. Phys.* 1957, 28, 1246.
- (62) Chapman, G. E.; Formery, B. W.; Thompson, M. W.; Wilson, J. H. *Radiat. Eff.* 1972, 13, 121.
- (63) Blaise, G.; Slodzian, G. *Rev. Phys. Appl.* 1973, 8, 105.
- (64) Rudat, M. A.; Morrison, G. H. *Surf. Sci.* 1979, 82, 549.
- (65) Vasile, M. J. *Phys. Rev. B: Condens. Matter* 1984, 29, 3785.
- (66) Benninghoven, A. *Surf. Sci.* 1973, 35, 427.
- (67) Wittmaack, K. *Surf. Sci.* 1981, 112, 168.
- (68) Andersen, C. A. *Int. J. Mass Spectrom. Ion Phys.* 1970, 3, 413.
- (69) Andersen, C. A.; Hinthorne, J. R. *Anal. Chem.* 1973, 45, 1421.
- (70) Morgan, A. E.; Werner, H. W. *Anal. Chem.* 1976, 48, 699.
- (71) Nørskov, J. K.; Lundqvist, B. I. *Phys. Rev. B: Condens. Matter* 1979, 19, 5661.
- (72) Garrison, B. J.; Winograd, N. *Chem. Phys. Lett.* 1983, 97, 381.
- (73) Oechsner, H. *Appl. Phys.* 1975, 8, 185.
- (74) McCracken, G. M. *Rep. Prog. Phys.* 1975, 38, 241.
- (75) Winters, H. F. In *Radiation Effects on Solid Surfaces*; Kaminsky, M., Ed.; Advances in Chemistry Series 158; American Chemical Society: Washington, DC, 1976; p 1.
- (76) Blaise, G.; Nourtier, A. *Surf. Sci.* 1979, 90, 495.
- (77) Williams, P. *Surf. Sci.* 1979, 90, 588.
- (78) Werner, H. W. *SIA, Surf. Interface Anal.* 1980, 2, 56.
- (79) Greene, J. E. *CRC Crit. Rev. Solid State Mater. Sci.* 1983, 11, 47.
- (80) Bernhardt, F.; Oechsner, H.; Stumpe, E. *Nucl. Instrum. Methods* 1976, 132, 329.
- (81) Kelly, R. *Radiat. Eff.* 1977, 32, 91.
- (82) Sigmund, P.; Claussen, C. J. *Appl. Phys.* 1981, 52, 990.
- (83) Magee, C. W. *Int. J. Mass Spectrom. Ion Phys.* 1983, 49, 211.
- (84) Schultz, J. A.; Kumar, R.; Rabalais, J. W. *Chem. Phys. Lett.* 1983, 100, 214.
- (85) Rabalais, J. W.; Chen, J.-N. *J. Chem. Phys.* 1986, 85, 3615.
- (86) Thompson, M. W. *Philos. Mag.* 1968, 18, 377.
- (87) Sigmund, P. *Phys. Rev.* 1969, 184, 383; 1969, 187, 768.
- (88) Sigmund, P. In *Sputtering by Particle Bombardment I*; Behrisch, R., Ed.; Topics in Applied Physics 47; Springer-Verlag: Berlin, 1981; p 9.
- (89) Garrison, B. J.; Winograd, N. *Science (Washington, D.C., 1883-)* 1982, 216, 805.
- (90) Falcone, G. *Phys. Rev. B: Condens. Matter* 1986, 33, 5054.
- (91) Szymonski, M.; Huang, W.; Onsgaard, J. *Nucl. Instrum. Methods Phys. Res., Sect. B* 1986, 14, 263.
- (92) Winograd, N. In *Desorption Mass Spectrometry*; Lyon, P. A., Ed.; ACS Symposium Series 291; American Chemical Society: Washington, DC, 1985; p 83.
- (93) Kimmock, F. M.; Baxter, J. P.; Pappas, D. L.; Kobrin, P. H.; Winograd, N. *Anal. Chem.* 1984, 56, 2782.
- (94) Müller, K.-H.; Seifert, K.; Wilmers, M. *J. Vac. Sci. Technol., A*, 1985, 3, 1367.
- (95) Lipinsky, D.; Jede, R.; Ganschow, O.; Benninghoven, A. *J. Vac. Sci. Technol., A* 1985, 3, 2007.
- (96) Jones, K. W.; Kramer, H. W. *Phys. Rev. A* 1975, 11, 1347.
- (97) Slodzian, G. *Surf. Sci.* 1975, 48, 161.
- (98) Gnaser, H. *Int. J. Mass Spectrom. Ion Processes* 1984, 61, 81.
- (99) Poole, R. T.; Jenkin, J. G.; Liesegang, J.; Leckey, R. C. G. *Phys. Rev. B: Solid State* 1975, 11, 5179.
- (100) Williams, P.; Evans, C. A., Jr. *Surf. Sci.* 1978, 78, 324.
- (101) Williams, P. *Int. J. Mass Spectrom. Ion Phys.* 1983, 53, 101.
- (102) Thomas, G. E. *Radiat. Eff.* 1977, 31, 185.
- (103) Blaise, G.; Slodzian, G. *Surf. Sci.* 1973, 40, 708.
- (104) Van der Weg, W. F.; Bierman, D. J. *Physica* 1969, 44, 206.
- (105) Kelly, R.; Kerkdijk, C. B. *Surf. Sci.* 1974, 46, 537.
- (106) Boudewijn, P. R.; Akerboom, H. W. P.; Kempener, M. N. C. *Spectrochim. Acta, Part B* 1984, 39, 1567.
- (107) Morgan, A. E.; Werner, H. W. *Anal. Chem.* 1977, 49, 927.
- (108) Coles, J. N. *Surf. Sci.* 1979, 79, 549.
- (109) Falcone, G.; Oliva, A. *Nucl. Instrum. Methods Phys. Res., Sect. B* 1984, 2, 697.
- (110) Yu, M. L.; Lang, N. D. *Nucl. Instrum. Methods Phys. Res., Sect. B* 1986, 14, 403.
- (111) Yu, M. L.; Lang, N. D. *Phys. Rev. Lett.* 1983, 50, 127.
- (112) Yu, M. L. *Phys. Rev. Lett.* 1981, 47, 1325.
- (113) Goldberg, E. C.; Ferrón, J.; Passeggi, M. C. G. *Phys. Rev. B: Condens. Matter* 1984, 30, 2448.
- (114) Yu, M. L.; Mann, K. *Phys. Rev. Lett.* 1986, 57, 1476.
- (115) Stroubek, Z. *Phys. Rev. B: Condens. Matter* 1982, 25, 6046.
- (116) Lin, J.-H.; Garrison, B. J. *J. Vac. Sci. Technol., A* 1983, 1, 1205.
- (117) Veksler, V. I. *Radiat. Eff.* 1980, 51, 129.
- (118) Garrison, B. J.; Winograd, N.; Harrison, D. E., Jr. *J. Chem. Phys.* 1978, 69, 1440.
- (119) Winograd, N.; Harrison, D. E., Jr.; Garrison, B. J. *Surf. Sci.* 1978, 78, 467.
- (120) Kimock, F. M.; Baxter, J. P.; Winograd, N. *Surf. Sci.* 1983, 124, L41.
- (121) Pargellis, A.; Seidl, M. *J. Vac. Sci. Technol., A* 1983, 1, 1388.
- (122) Bernheim, M.; Blaise, G.; Slodzian, G. *Int. J. Mass Spectrom. Ion Phys.* 1972/1973, 10, 293.
- (123) Williams, P. *Nucl. Instrum. Methods Phys. Res., Sect. B* 1986, 15, 159.
- (124) Brochard, D.; Slodzian, G. *J. Phys.* 1971, 32, 185.
- (125) *CRC Handbook of Chemistry and Physics*, 61st ed.; Weast, R. C., Ed.; CRC: Boca Raton, FL, 1980.
- (126) Dillon, A. F.; Lehrle, R. S.; Robb, J. C.; Thomas, D. W. *Adv. Mass Spectrom.* 1968, 4, 477.
- (127) Benninghoven, A. *Z. Phys.* 1970, 230, 403.
- (128) Harrison, D. E., Jr.; Moore, W. L., Jr.; Holcombe, H. T. *Radiat. Eff.* 1973, 17, 167.
- (129) Harrison, D. E., Jr.; Delaplain, C. B. *J. Appl. Phys.* 1976, 47, 2252.
- (130) Garrison, B. J. *Int. J. Mass Spectrom. Ion Phys.* 1983, 53, 243.
- (131) Winograd, N.; Garrison, B. J.; Harrison, D. E., Jr. *J. Chem. Phys.* 1980, 73, 3473.

- (132) Lauderback, L. L.; Delgass, W. N. *Phys. Rev. B: Condens. Matter* **1982**, *26*, 5258.
- (133) Garrison, B. J. *J. Am. Chem. Soc.* **1980**, *102*, 6553.
- (134) Garrison, B. J. *J. Am. Chem. Soc.* **1982**, *104*, 6211.
- (135) Winograd, N.; Karwacki, E. J. *Anal. Chem.* **1983**, *55*, 790.
- (136) Jonkman, H. T.; Michl, J.; King, R. N.; Andrade, J. D. *Anal. Chem.* **1978**, *50*, 2078.
- (137) Lancaster, G. M.; Honda, F.; Fukuda, Y.; Rabalais, J. W. *J. Am. Chem. Soc.* **1979**, *101*, 1951.
- (138) Moon, D. W.; Winograd, N. *Int. J. Mass Spectrom. Ion Phys.* **1983**, *52*, 217.
- (139) Keiner, L.; Markey, S. P. *Int. J. Mass Spectrom. Ion Processes* **1984**, *59*, 157.
- (140) Benninghoven, A. *Int. J. Mass Spectrom. Ion Phys.* **1983**, *53*, 85.
- (141) Ishitani, T.; Shimizu, R. *Phys. Lett.* **1974**, *46A*, 487.
- (142) Benninghoven, A. *Surf. Sci.* **1975**, *53*, 596.
- (143) Lange, W.; Holtkamp, D.; Jirikowsky, M.; Benninghoven, A. In *Ion Formation from Organic Solids*; Benninghoven, A., Ed.; Springer Series in Chemical Physics 25; Springer-Verlag: Berlin, 1983; p 124.
- (144) Lange, W.; Jirikowsky, M.; Benninghoven, A. *Surf. Sci.* **1984**, *136*, 419.
- (145) Benninghoven, A. *J. Vac. Sci. Technol.*, **A** **1985**, *3*, 451.
- (146) Holtkamp, D.; Jirikowsky, M.; Kempken, M.; Benninghoven, A. *J. Vac. Sci. Technol.*, **A** **1985**, *3*, 1394.
- (147) Jonkman, H. T.; Michl, J. *J. Am. Chem. Soc.* **1981**, *103*, 733.
- (148) Orth, R. G.; Jonkman, H. T.; Powell, D. H.; Michl, J. *J. Am. Chem. Soc.* **1981**, *103*, 6026.
- (149) Orth, R. G.; Jonkman, H. T.; Michl, J. *J. Am. Chem. Soc.* **1982**, *104*, 1834.
- (150) Orth, R. G.; Jonkman, H. T.; Michl, J. *Int. J. Mass Spectrom. Ion Phys.* **1982**, *43*, 41.
- (151) Stulik, D.; Orth, R. G.; Jonkman, H. T.; Michl, J. *Int. J. Mass Spectrom. Ion Phys.* **1983**, *53*, 341.
- (152) Liang, J.; Michl, J. *J. Am. Chem. Soc.* **1984**, *106*, 5039.
- (153) Magnera, T. F.; David, D. E.; Tian, R.; Stulik, D.; Michl, J. *J. Am. Chem. Soc.* **1984**, *106*, 5040.
- (154) David, D. E.; Magnera, T. F.; Tian, R.; Michl, J. *Radiat. Eff.* **1986**, *99*, 247.
- (155) Michl, J. *Int. J. Mass Spectrom. Ion Phys.* **1983**, *53*, 255.
- (156) David, D. E.; Magnera, T. F.; Tian, R.; Stulik, D.; Michl, J. *Nucl. Instrum. Methods Phys. Res., Sect. B* **1986**, *14*, 378.
- (157) Urbassek, H. M.; Michl, J. *Nucl. Instrum. Methods Phys. Res., Sect. B*, in press.
- (158) Brown, W. L.; Johnson, R. E. *Nucl. Instrum. Methods Phys. Res., Sect. B* **1986**, *13*, 295.
- (159) Magnera, T. F.; David, D. E.; Michl, J. *Chem. Phys. Lett.* **1986**, *123*, 327.
- (160) Busch, K. L.; Hsu, B. H.; Xie, Y.-X.; Cooks, R. G. *Anal. Chem.* **1983**, *55*, 1157.
- (161) Liu, L. K.; Busch, K. L.; Cooks, R. G. *Anal. Chem.* **1981**, *53*, 109.
- (162) Unger, S. E.; Day, R. J.; Cooks, R. G. *Int. J. Mass Spectrom. Ion Phys.* **1981**, *39*, 231.
- (163) Busch, K. L.; Cooks, R. G. *Science (Washington, D.C., 1883-)* **1982**, *218*, 247.
- (164) Cooks, R. G.; Busch, K. L. *Int. J. Mass Spectrom. Ion Phys.* **1983**, *53*, 111.
- (165) Busch, K. L.; Hsu, B. H.; Xie, Y.-X.; Cooks, R. G. In *Ion Formation from Organic Solids*; Benninghoven, A., Ed.; Springer Series in Chemical Physics 25; Springer-Verlag: Berlin, 1983; p 138.
- (166) Zakett, D.; Schoen, A. E.; Cooks, R. G.; Hemberger, P. H. *J. Am. Chem. Soc.* **1981**, *103*, 1295.
- (167) Pachuta, S. J.; Cooks, R. G. In *Desorption Mass Spectrometry*; Lyon, P. A., Ed.; ACS Symposium Series 291; American Chemical Society: Washington, DC, 1985; p 1.
- (168) Hsu, B. H.; Cooks, R. G. *Anal. Chem.* **1985**, *57*, 2925.
- (169) Ross, M. M.; Colton, R. J. *Anal. Chem.* **1983**, *55*, 150.
- (170) Alai, M.; Demirev, P.; Fenselau, C.; Cotter, R. J. *Anal. Chem.* **1986**, *58*, 1303.
- (171) Hsu, B.-H.; Xie, X.-Y.; Busch, K. L.; Cooks, R. G. *Int. J. Mass Spectrom. Ion Phys.* **1983**, *51*, 225.
- (172) Cooks, R. G.; Hsu, B.-H.; Emary, W. B.; Fife, W. K. In *Ion Formation from Organic Solids (IFOS III)*; Benninghoven, A., Ed.; Springer Proceedings in Physics 9; Springer-Verlag: Berlin, 1986; p 28.
- (173) Wong, S. S.; Röllgen, F. W.; Manz, I.; Przybylski, M. *Biomed. Mass Spectrom.* **1985**, *12*, 43.
- (174) McLafferty, F. W., Ed. *Tandem Mass Spectrometry*; Wiley: New York, 1983.
- (175) Pierce, J. L.; Busch, K. L.; Cooks, R. G.; Walton, R. A. *Inorg. Chem.* **1982**, *21*, 2597.
- (176) Busch, K. L.; Cooks, R. G.; Walton, R. A.; Wood, K. V. *Inorg. Chem.* **1984**, *23*, 4093.
- (177) Glish, G. L.; Todd, P. J.; Busch, K. L.; Cooks, R. G. *Int. J. Mass Spectrom. Ion Processes* **1984**, *56*, 177.
- (178) Crow, F. W.; Tomer, K. B.; Gross, M. L.; McCloskey, J. A.; Bergstrom, D. E. *Anal. Biochem.* **1984**, *139*, 243.
- (179) Unger, S. E. *Int. J. Mass Spectrom. Ion Processes* **1985**, *66*, 195.
- (180) Carr, S. A.; Reinhold, V. N.; Green, B. N.; Hass, J. R. *Biomed. Mass Spectrom.* **1985**, *12*, 288.
- (181) Keough, T. *Anal. Chem.* **1985**, *57*, 2027.
- (182) Ens, W.; Beavis, R.; Standing, K. G. *Phys. Rev. Lett.* **1983**, *50*, 27.
- (183) Baldwin, M. A.; Proctor, C. J.; Amster, I. J.; McLafferty, F. W. *Int. J. Mass Spectrom. Ion Processes* **1983**, *54*, 97.
- (184) Campana, J. E.; Green, B. N. *J. Am. Chem. Soc.* **1984**, *106*, 531.
- (185) Chait, B. T.; Field, F. H. *Int. J. Mass Spectrom. Ion Phys.* **1981**, *41*, 17.
- (186) Chait, B. T.; Field, F. H. *Int. J. Mass Spectrom. Ion Processes* **1985**, *65*, 169.
- (187) Della-Negra, S.; LeBeyec, Y. *Anal. Chem.* **1985**, *57*, 2035.
- (188) Didonato, G. C.; Busch, K. L. *Int. J. Mass Spectrom. Ion Processes* **1986**, *69*, 67.
- (189) Wandass, J. H.; Gardella, J. A., Jr. *J. Am. Chem. Soc.* **1985**, *107*, 6192.
- (190) Hsu, B.-H.; Cooks, R. G. *Anal. Chem.* **1985**, *57*, 2925.
- (191) Unger, S. E.; Cooks, R. G.; Steinmetz, B. J.; Delgass, W. N. *Surf. Sci.* **1982**, *116*, L211.
- (192) Detter, L. D.; Walton, R. A.; Cooks, R. G. *Inorg. Chem. Acta* **1986**, *115*, 55.
- (193) Aberth, W.; Straub, K. M.; Burlingame, A. L. *Anal. Chem.* **1982**, *54*, 2029.
- (194) Brown, A.; van den Berg, J. A.; Vickerman, J. C. *J. Chem. Soc., Chem. Commun.* **1984**, 1684.
- (195) Van der Peyl, G. J. Q.; Van der Zande, W. J.; Hoogerbrugge, R.; Kistemaker, P. G. *Int. J. Mass Spectrom. Ion Processes* **1985**, *67*, 147.
- (196) Campana, J. E.; Dunlap, B. *Int. J. Mass Spectrom. Ion Processes* **1984**, *57*, 103.
- (197) Cook, K. D.; Chan, K. W. S. *Int. J. Mass Spectrom. Ion Processes* **1983**, *54*, 135.
- (198) Ligon, W. V., Jr. *Int. J. Mass Spectrom. Ion Phys.* **1983**, *52*, 183.
- (199) Wong, S. S.; Röllgen, F. W. *Nucl. Instrum. Methods Phys. Res., Sect. B* **1986**, *14*, 436.
- (200) Bursey, M. M.; Marbury, G. D.; Hass, J. R. *Biomed. Mass Spectrom.* **1984**, *11*, 522.
- (201) Lehmann, W. D.; Kessler, M.; König, W. A. *Biomed. Mass Spectrom.* **1984**, *11*, 217.
- (202) Gower, J. L. *Biomed. Mass Spectrom.* **1985**, *12*, 191.
- (203) Ligon, W. V., Jr. *Int. J. Mass Spectrom. Ion Phys.* **1983**, *52*, 189.
- (204) Martin, S. A.; Costello, C. E.; Biemann, K. *Anal. Chem.* **1982**, *54*, 2362.
- (205) Puzo, G.; Prome, J.-C. *Org. Mass Spectrom.* **1984**, *19*, 448.
- (206) DePauw, E. *Mass Spectrom. Rev.* **1986**, *5*, 191.
- (207) Groenewold, G. S.; Todd, P. J.; Buchanan, M. V. *Anal. Chem.* **1984**, *56*, 2251.
- (208) Ligon, W. V., Jr. *Int. J. Mass Spectrom. Ion Phys.* **1983**, *52*, 189.
- (209) Field, F. H. *J. Phys. Chem.* **1982**, *86*, 5115.
- (210) Cooper, R.; Unger, S. *J. Antibiot.* **1985**, *38*, 24.
- (211) Schiebel, H.-M.; Schulze, P.; Stohrer, W.-D.; Leibfritz, D.; Jastorff, B.; Maurer, K. H. *Biomed. Mass Spectrom.* **1985**, *12*, 170.
- (212) Sunner, J. A.; Kulatunga, R.; Kebarle, P. *Anal. Chem.* **1986**, *58*, 1312.
- (213) Macfarlane, R. D. *Acc. Chem. Res.* **1982**, *15*, 268.
- (214) Sundqvist, B.; Hedin, A.; Håkansson, P.; Kamensky, I.; Salehpour, M.; Säwe, G. *Int. J. Mass Spectrom. Ion Processes* **1985**, *65*, 69.
- (215) Blauner, P. G.; O'Connor, J. P.; Weller, R. A. *Nucl. Instrum. Methods Phys. Res., Sect. B* **1985**, *12*, 343.
- (216) Macfarlane, R. D. In *Desorption Mass Spectrometry*; Lyon, P. A., Ed.; ACS Symposium Series 291; American Chemical Society: Washington, DC, 1985; p 56.
- (217) Ens, W.; Standing, K. G.; Chait, B. T.; Field, F. H. *Anal. Chem.* **1981**, *53*, 1241.
- (218) Kamensky, I.; Håkansson, P.; Sundqvist, B.; McNeal, C. J.; Macfarlane, R. D. *Nucl. Instrum. Methods* **1982**, *198*, 65.
- (219) Salehpour, M.; Håkansson, P.; Sundqvist, B.; Widdiyasekera, S. *Nucl. Instrum. Methods Phys. Res., Sect. B* **1986**, *13*, 278.
- (220) Håkansson, P.; Jayasinghe, E.; Johansson, A.; Kamensky, I.; Sundqvist, B. *Phys. Rev. Lett.* **1981**, *47*, 1227.
- (221) Macfarlane, R. D.; Torgerson, D. F. *Phys. Rev. Lett.* **1976**, *36*, 486.
- (222) Brown, W. L.; Lanzerotti, L. J.; Poate, J. M.; Augustyniak, W. M. *Phys. Rev. Lett.* **1978**, *40*, 1027.
- (223) Seiberling, L. E.; Griffith, J. E.; Tombrello, T. A. *Radiat. Eff.* **1980**, *52*, 201.
- (224) Brown, W. L.; Augustyniak, W. M.; Lanzerotti, L. J.; Johnson, R. E.; Evatt, R. *Phys. Rev. Lett.* **1980**, *45*, 1632.
- (225) Besenbacher, F.; Böttiger, J.; Graversen, O.; Hansen, J. L.; Sørensen, H. *Nucl. Instrum. Methods* **1981**, *191*, 221.
- (226) Lucchese, R. R. *J. Chem. Phys.*, in press.

- (227) Beuhler, R. J.; Flanigan, E.; Greene, L. J.; Friedman, L. J. *Am. Chem. Soc.* 1974, 96, 3990.
- (228) Johnson, R. E.; Sundqvist, B. *Int. J. Mass Spectrom. Ion Phys.* 1983, 53, 337.
- (229) Hedin, A.; Håkansson, P.; Sundqvist, B.; Johnson, R. E. *Phys. Rev. B: Condens. Matter* 1985, 31, 1780.
- (230) Sundqvist, B.; Hedin, A.; Håkansson, P.; Salehpour, M.; Säve, G.; Johnson, R. E. *Nucl. Instrum. Methods Phys. Res., Sect. B* 1986, 14, 429.
- (231) Jonsson, G. P.; Hedin, A. B.; Håkansson, P. L.; Sundqvist, B.; Säve, B. G.; Nielsen, P. F.; Roepstorff, P.; Johansson, K.-E.; Kamensky, I.; Lindberg, M. S. L. *Anal. Chem.* 1986, 58, 1084.
- (232) Balasanmugam, K.; Dang, T. A.; Day, R. J.; Hercules, D. M. *Anal. Chem.* 1981, 53, 2296.
- (233) Hercules, D. M.; Day, R. J.; Balasanmugam, K.; Dang, T. A.; Li, C. P. *Anal. Chem.* 1982, 54, 280A.
- (234) Novak, F. P.; Balasanmugam, K.; Viswanadham, K.; Parker, C. D.; Wilk, Z. A.; Mattern, D.; Hercules, D. M. *Int. J. Mass Spectrom. Ion Phys.* 1983, 53, 135.
- (235) Dang, T. A.; Day, R. J.; Hercules, D. M. *Anal. Chim. Acta* 1984, 158, 235.
- (236) Hillenkamp, F. In *Ion Formation from Organic Solids*; Benninghoven, A., Ed.; Springer Series in Chemical Physics 25; Springer-Verlag: Berlin, 1982; p 190.
- (237) Jöst, B.; Schueler, B.; Krueger, F. R. *Z. Naturforsch., A: Phys., Phys. Chem., Kosmophys.* 1982, 37, 18.
- (238) Hillenkamp, F.; Karas, M.; Rosmarinowsky, J. In *Desorption Mass Spectrometry*; Lyon, P. A., Ed.; ACS Symposium Series 291; American Chemical Society: Washington, DC, 1985; p 69.
- (239) Vastola, F. J.; Pirone, A. J. *Adv. Mass Spectrom.* 1968, 4, 107.
- (240) Cotter, R. J. *Anal. Chem.* 1980, 52, 1770.
- (241) Cotter, R. J. *Trends Anal. Chem.* 1982, 1, 307.
- (242) Van Breeman, R. B.; Snow, M.; Cotter, R. J. *Int. J. Mass Spectrom. Ion Phys.* 1983, 49, 35.
- (243) Tabet, J.-C.; Cotter, R. J. *Int. J. Mass Spectrom. Ion Processes* 1983, 54, 151.
- (244) Tabet, J.-C.; Cotter, R. J. *Anal. Chem.* 1984, 56, 1662.
- (245) Tabet, J.-C.; Jablonski, M.; Cotter, R. J.; Hunt, J. E. *Int. J. Mass Spectrom. Ion Processes* 1985, 65, 105.
- (246) Van der Peyl, G. J. Z.; Haverkamp, J.; Kistemaker, P. G. *Int. J. Mass Spectrom. Ion Phys.* 1982, 42, 125.
- (247) Stoll, R.; Röllgen, F. W. *J. Chem. Soc., Chem. Commun.* 1980, 789.
- (248) Stoll, R.; Röllgen, F. W. *Org. Mass Spectrom.* 1981, 16, 72.
- (249) Van der Peyl, G. J. Z.; Isa, K.; Haverkamp, J.; Kistemaker, P. G. *Int. J. Mass Spectrom. Ion Phys.* 1981, 16, 416.
- (250) Stoll, R.; Röllgen, F. W. *Z. Naturforsch., A Phys., Phys. Chem., Kosmophys.* 1982, 37, 9.
- (251) Egorov, S. E.; Letokhov, V. S.; Shibano, A. N. In *Surface Studies with Lasers*; Aussenegg, F. R., Leitner, A., Lippitsch, M. E., Eds.; Springer Series in Chemical Physics 33; Springer-Verlag: Berlin, 1984; p 156.
- (252) Bojeson, G.; Möller, J. *Int. J. Mass Spectrom. Ion Processes* 1986, 68, 239.
- (253) Emary, W. B.; Isern-Flecha, I.; Wood, K. V.; Ridley, R. Y.; Cooks, R. G. *Talanta*, in press.
- (254) Harden, E. D.; Vestal, M. L. *Anal. Chem.* 1981, 53, 1492.
- (255) Mauney, T.; Adams, F. *Int. J. Mass Spectrom. Ion Processes* 1984, 59, 103.
- (256) Van der Peyl, G. J. Z.; Van der Zande, W. J.; Kistemaker, P. G. *Int. J. Mass Spectrom. Ion Processes* 1984, 62, 51.
- (257) Fürstenau, N.; Hillenkamp, F. *Int. J. Mass Spectrom. Ion Phys.* 1981, 37, 135.
- (258) Davis, D. V.; Cooks, R. G.; Meyer, B. N.; McLaughlin, J. L. *Anal. Chem.* 1983, 55, 1302.
- (259) Wright, L. G.; Cooks, R. G.; Wood, K. V. *Biomed. Mass Spectrom.* 1985, 12, 159.
- (260) Vestal, M. L. *Mass Spectrom. Rev.* 1983, 2, 447.
- (261) Krueger, F. R. *Z. Naturforsch., A Phys., Phys. Chem., Kosmophys.* 1983, 38, 385.
- (262) Kissel, J.; Krueger, F. R. *Appl. Phys. A* 1987, 42, 69.
- (263) Ziv, A. R.; King, B. V.; Lin, S. H.; Tsong, I. S. T. *Nucl. Instrum. Methods Phys. Res.* 1983, 218, 742.
- (264) King, B. V.; Ziv, A. R.; Lin, S. H.; Tsong, I. S. T. *J. Chem. Phys.* 1985, 82, 3641.
- (265) Forst, W. *Theory of Unimolecular Reactions*; Academic: New York, 1973.